THE JOURNAL OF PHYSICAL CHEMISTRY B

pubs.acs.org/JPCB

Article

N-Terminal Decarboxylation as a Probe for Intramolecular Contact Formation in γ-Glu-(Pro)$_n$-Met Peptides

Piotr Filipiak,* Krzysztof Bobrowski, Gordon L. Hug, Christian Schöneich, and Bronislaw Marciniak

Cite This: *J. Phys. Chem. B* 2020, 124, 8082–8098

Read Online

ACCESS | Metrics & More | Article Recommendations | Supporting Information

ABSTRACT: The kinetics of intramolecular-contact formation between remote functional groups in peptides with restricted conformational flexibility were examined using designed peptides with variable-length proline bridges. As probes for this motion, free radicals were produced using the $^{\bullet}$OH-induced oxidation at the C-terminal methionine residue of γ-Glu-(Pro)$_n$-Met peptides (n = 0–3). The progress of the radicals' motion along the proline bridges was monitored as the radicals underwent reactions along the peptides' backbones. Of particular interest was the reaction between the sulfur atom located in the side chain of the oxidized Met residue and the unprotonated amino group of the glutamic acid moiety. Interactions between them were probed by the radiation-chemical yields (expressed as G values) of the formation of C-centered, α-aminoalkyl radicals (αN) on the Glu residue. These radicals were monitored directly or via their reaction with p-nitroacetophenone (PNAP) to generate the optically detected PNAP$^{\bullet-}$ radical anions. The yields of these αN radicals were found to be linearly dependent on the number of Pro residues. A constant decrease by 0.09 μM J^{-1} per spacing Pro residue of the radiation-chemical yields of G(αN) was observed. Previous reports support the conclusion that the αN radicals in these cases would have to result from (S∴N)$^+$-bonded cyclic radical cations that arose as a result from direct contact between the ends of the peptides. Furthermore, by analogy with the rate constants for the formation of intramolecularly (S∴S)$^+$-bonded radical cations in Met-(Pro)$_n$-Met peptides (*J. Phys. Chem. B* **2016**, *120*, 9732), the rate constants for the formation of intramolecularly (S∴N)$^+$-bonded radical cations are activated to the same extent for all of the γ-Glu-(Pro)$_n$-Met peptides. Thus, the continuous decrease of G(αN) with the number of Pro residues (from 0 to 3) suggests that the formation of a contact between the S-atom in the C-terminal Met residue and the N-atom of a deprotonated N-terminal amino group of Glu is controlled in peptides with 0 to 3 Pro residues by the relative diffusion of the S$^{\bullet+}$ and unoxidized N-atom. The overall rate constants of cyclization to form the (S∴N)-bonded radical cations were estimated to be 3.8 × 10^6, 1.8 × 10^6, and 8.1 × 10^5 s^{-1} for peptides with n = 0, 1, and 2 Pro residues, respectively. If activation is the same for all of the peptides, then these rate constants are a direct indication for the end-to-end dynamics along the chain.

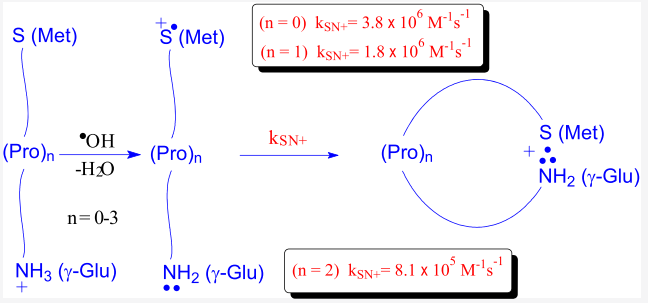

1. INTRODUCTION

The efficiency and time scales of intramolecular-contact formation between remote functional groups located on the opposite ends of an unfolded polypeptide backbone are important for polypeptide dynamics characteristics. This is essential for the understanding of protein folding, leading to stable structures,[1−3] and for long-distance electron and proton transfer processes in proteins.[4,5] For many years, such studies have generally employed stopped-flow techniques, which are limited to millisecond or longer time scales, and therefore, early events cannot be observed.[6−8] Some improvement in time resolution to submilliseconds was achieved by ultrarapid mixing to study the folding of cytochrome c either by combination with resonance Raman spectroscopy[9] or by using quenching of tryptophan fluorescence by the heme in the previously inaccessible time range of 80 μs to 3 ms.[10] On the other hand, relaxation methods such as temperature jump,[11] and laser-induced temperature jump,[12−16] pressure jump,[17] electric jump,[18] and resonant ultrasounds[19] that can access the nanosecond time scale did not give an unequivocal structural assignment of the kinetics because of interference from molecular reorientation, solvation, charge transfer, and proton-transfer reactions.

For the above reasons, it was advisable to develop other methods that can initiate protein folding. The first successful experiments were performed by using the so-called "photochemical triggering" approach when the folding of reduced cytochrome c was initiated by its photodissociation. The intramolecular methionine binding at the heme iron after CO dissociation in unfolded cytochrome c was one of the first

Received: May 15, 2020
Revised: August 19, 2020
Published: August 19, 2020

https://dx.doi.org/10.1021/acs.jpcb.0c04371
J. Phys. Chem. B 2020, 124, 8082–8098

attempts to study the kinetics of contact formation.[20] Using time-resolved spectroscopy, formation of both (Met^{80}) and non-native (Met^{65}, His^{33}, and His^{26}) complexes with the heme iron at His^{18} occurs in ≈40 μs (for Met complexes) and ≈400 μs (for His complexes), even though the His residue is positioned closer to the heme. The measured binding rate ($\sim 2.5 \times 10^4$ s^{-1}) was taken as the rate of forming a contact between sites (Met^{65}/Met^{80}) located by about 50−60 residues along the sequence from the heme.[21] This value was taken as the intrachain diffusion rate. Based on the theory of Thirumalai and co-workers[22] that the fastest forming loops are formed 30- to 40-fold faster than loops of 50−60 residues, the upper limit for the rate of formation of the smallest intrachain loops in a polypeptide was calculated to be $\sim 10^6$ s^{-1}.[23]

In the next approach, a direct measure of intramolecular contact was obtained by the determination of triplet-triplet energy transfer between thioxanthone and naphthalene attached at defined points in flexible peptides containing repeating units of glycine and serine. In that case, energy transfer proceeds by the Dexter mechanism that requires van der Waals contact between the donor and acceptor. The rate of thioxanthone triplet decay was taken as the rate of contact formation. The rate of contact formation decreased with increasing number of peptide bonds separating the donor and acceptor and reached a value of 1.4×10^7 s^{-1} for the longest peptide with a donor and an acceptor separated by 12 peptide bonds.[24]

Another method for studying contact formation was based on measurements of the lifetime of the tryptophan triplet state (^{3}Trp) in flexible peptides with tryptophan (Trp) at one end and cysteine (Cys) at the other. Because Cys is an efficient quencher of ^{3}Trp, the rate of forming a contact between the side chains of Trp and Cys in a polypeptide is very close to the measured decay rate of ^{3}Trp. The peptides studied separating Trp and Cys consisted of multiples of the sequence (Ala-Gly-Gln)$_k$ with k varying from 1 to 6. It was found that the rate of quenching decreases from 2.5×10^7 s^{-1} for k = 1 to 7.2×10^6 s^{-1} for k = 6.[25] By measuring the viscosity dependence of the quenching rate, both the reaction-limited and diffusion-limited quenching rates were determined. The diffusion-limited rate corresponds to the rate of forming a short-range contact.[26]

A similar approach was used to determine the end-to-end contact of the coiled state of a 22 residue helix-forming peptide, which consisted of four peptide segments (Ala-Ala-Arg-Ala-Ala) separating a C-terminal Trp residue and an N-terminal lipoic acid moiety as a quencher of ^{3}Trp. Analysis of the decay of ^{3}Trp yields the diffusion-limited end-to-end contact rate of 1.1×10^7 s^{-1}.[27] In order to make a direct comparison of the effect of sequence, the rate for the same decay in a 22-residue peptide (in which all of Ala residues were replaced by threonine (Thr) residues and Cys was used instead of lipoate) was found to be 10-fold smaller (1.1×10^6 s^{-1}).[27] In order to understand the origin of these differences in rates, the theory of Szabo, Schulten, and Schulten (SSS) for end-to-end contact of polymer chains was applied.[28] According to the SSS theory, the mean first passage time for end-to-end contact depends simply on the relative end-to-end diffusion coefficient (D) and the root-mean-squared end-to-end distance (r^2). Threonine may decrease D and therefore decrease the rate by increasing barriers to dihedral angle motion, and its bulkier side-chain compared to Ala could slow the rate by increasing r^2.[27]

Other interesting examples of using the technique of Trp-Cys contact quenching were the measurements of the rate of intramolecular contact in four different loops along the chain in α-synuclein,[29] in a fragment of human prostatic acidic phosphatase (PAP) showing that the full-length peptide diffuses much faster than the truncated peptide,[30] in protein L showing surprisingly low diffusion rates,[31,32] and in Syrian hamster and rabbit prion proteins at different pH values and concentration of denaturants.[33]

The results presented above showed that some directly induced photochemical processes can be used for studying the kinetics of intramolecular-contact formation in peptides and proteins.

In the mid-1990s, $^{\bullet}$OH-induced side-chain fragmentation of threonine (Thr) and serine (Ser) residues to the respective aldehydes in Ser-Met and Thr-Met dipeptides was explained by an intramolecular interaction through a direct contact of a deprotonated N-terminal amino group with the sulfur radical site in the side chain of the C-terminal methionine (Met) residue,[34] and later in the early 2000s in Thr-(Gly)$_n$-Met (n = 0−4) oligopeptides.[35] The same kind of interaction was proposed to explain N-terminal decarboxylation of glutamic acid (Glu) residue in γ-Glu-Met and γ-Glu-Gly-Met-Gly peptides and S-methylglutathione (γ-Glu-S-MeCys-Gly) and formation of α-aminoalkyl radicals.[36−38] In turn, the formation of intramolecularly S∴S-bonded radical cations in linear and cyclic Met-Met dipeptides was explained by the interaction of side chains of Met residues.[39,40] It was assumed that formation of such intramolecular contacts benefits from the conformational flexibility of peptides studied. These processes formed the basis of a new generation of kinetic experiments that are triggered by radicals, i.e., "radical triggering", and enable studies on kinetics of intramolecular-contact formation. The efficiency of intramolecular contact can be probed by the formation of specific transients or stable products.

The first attempt of studies on the kinetics and efficiency of contact formation were performed in Thr-(Pro)$_n$-Met (n = 0−4) oligopeptides, applying $^{\bullet}$OH radicals as the radical trigger.[35] The use of such peptides with restricted conformational flexibility allowed for a certain distance control between the amino acids located at N- and C-terminals. It was shown that, in Thr-(Pro)$_n$-Met (n = 0−4) oligopeptides, the efficiency of acetaldehyde formation (f) (defined as [acetaldehyde]/[consumed peptide]) was significantly decreased by an insertion of the first Pro residue from f = 0.21 to f = 0.05. Interestingly, there was no significant difference (within error limits) between f for oligopeptides containing 1 to 4 proline residues. A significant change in f can be explained by the restriction of conformational flexibility in Thr-(Pro)$_n$-Met (n = 1−4) in comparison to Thr-Met dipeptide. In turn, the small change in f for Thr-(Pro)$_n$-Met (n = 1−4) could be interpreted as a superposition of two opposite effects resulting from the different distance dependence of the two mechanisms of electron transfer.

Another method for studying kinetics of contact formation was based on measurements of the radiation-chemical yields (G values) of intramolecularly S∴S-bonded radical cations $(S\therefore S)^+$ in Met-(Pro)$_n$-Met (n = 0−4), applying $^{\bullet}$OH radicals,[41] and 4-carboxybenzophenone triplets as "radical triggers".[42] The yields of $(S\therefore S)^+$ were found to be dependent on the number of Pro residues. It should be noted that, in this case, the largest decrease in $G(S\therefore S)^+$ occurred when the number of Pro residues was changed from 2 to 3. These

https://dx.doi.org/10.1021/acs.jpcb.0c04371
J. Phys. Chem. B 2020, 124, 8082−8098

features were quantitatively analyzed by Langevin Dynamics[43] and a statistical mechanical SSS theory.[28] The analysis showed that the formation of contact between sulfur atoms located in terminal Met residues in the peptides with 0−2 Pro residues was controlled by the activated formation of $(S.\therefore S)^+$, whereas in the peptides with 3 and 4 Pro residues, by the relative diffusion of $>S^{\bullet+}$ and the unoxidized S-atom.

In the current study, we selected γ-Glu-$(Pro)_n$-Met (n = 0−3) oligopeptides that contain Glu and Met residues located on the N- and C-terminal, respectively, and that are separated by a defined number (0−3) of Pro residues. These peptides are characterized by the presence of an isopeptide bond between the γ-carboxyl group of the N-terminal Glu residue and the α-amino group of the Pro residue. In vivo, glutathione (an important antioxidant in plants, animals, and humans)[44] and S-alkylglutathiones (playing various functions in living organisms)[45−47] are examples of peptides with an isopeptide bond involving an N-terminal Glu residue.

The broad aim of this research was to test whether the kinetics of intramolecularly S.∴N-bonded radical cation formation could be used to follow end-to-end contact formation in oligopeptides. This S.∴N-bonded radical cation formation occurs via the well-known mechanism of $^{\bullet}$OH-induced oxidation of γ-Glu-Met,[36,48] γ-Glu-Gly-Met-Gly,[37] and S-methylglutathione.[36,38,49] The current work shows how this reaction can be used to monitor intramolecular-contact formation kinetics between a remote N-terminal amino group in a γ-Glu residue and an oxidized thioether group in a C-terminal Met residue in peptides with restricted conformational flexibility. Moreover, formation of other radicals (α-(alkylthio)alkyl, α-amidoalkyl, and SO-bonded radicals) that can form during the progress of the remote groups' motion along the proline bridges served also as a probe for the kinetics of this motion.

The basic idea of the experiment is that the intramolecularly S.∴N-bonded radical cation undergoes fast and efficient decarboxylation that leads at the same time to the formation of α-aminoalkyl radicals on the Glu residue. If formation of $(S.\therefore N)^+$ radical cations is not possible, then decarboxylation at the N-terminal of peptides studied would not occur. To demonstrate the utility of this method, we have investigated the simplest dynamical property of a polypeptide chain, i.e., the rate of end-to-end contact formation. We have used the reaction of p-nitroacetophenone (PNAP) with α-aminoalkyl radicals to determine their yields by measuring the yield of optically detected $PNAP^{\bullet-}$ radical anions. The experiments showed that the yields of α-aminoalkyl radicals decreased linearly with the number of Pro residues.

Though there are many proteins in vivo containing internal Glu residues that formed isopeptide bonds,[50,51] to the best of our knowledge, there are none with the Glu residue located at the N-terminal. On the other hand, there are several peptides of pharmaceutical interest[52] and proteins containing N-terminal Glu residues.[53−55] However, they are involved in the formation of an "ordinary" peptide bond. Despite this fact, some of these proteins can be used for studying the kinetics of intramolecular-contact formation by applying the approach in the current study; however, after prior modification of the type of peptide bond in which the N-terminal Glu residue is involved.

2. EXPERIMENTAL SECTION

2.1. Materials. γ-Glutamyl-Methionine (γ-Glu-Met) and γ-Glutamyl-$(Proline)_n$-Methionine, (γ-Glu-$(Pro)_1$-Met), (γ-Glu-$(Pro)_2$-Met), (γ-Glu-$(Pro)_3$-Met), were synthetized by the Biochemical Resource and Service Laboratory of the University of Kansas (see structures in Chart 1). They were purified to >95% purity and characterized by mass spectrometry.

Chart 1. Structures of γ-Glu-$(Pro)_n$-Met, n = 0−3; at Medium pH (3 < pH < 9), the N-Terminal Amine Is Protonated and the N- and C-Terminal Carboxyl Groups Are Deprotonated: H_3N^+− and COO^- (Anionic Form)

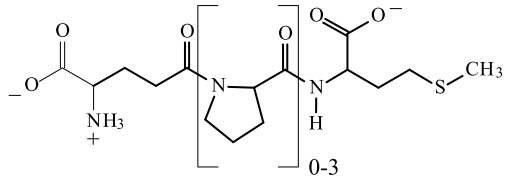

The other chemicals were obtained as follows: perchloric acid ($HClO_4$) was purchased from Aldrich Chemical Co. (Milwaukee, WI), reagent grade NaOH was obtained from J.T. Baker, and N-ethylacetamide was bought from Sigma-Aldrich.

Deionized water for time-resolved experiments (18 MΩ resistance) was purified in a reverse osmosis/deionization water system from Serv-A-Pure Co. The pH was adjusted by the addition of either NaOH or $HClO_4$. Solutions were subsequently purged for at least 30 min per 500 mL of sample with the desired gas (N_2O or N_2).

2.2. Pulse Radiolysis. The pulse radiolysis experiments were performed with the Notre Dame Titan 8 MeV Beta model TBS 8/16-1S linear accelerator with typical pulse lengths of 2.5−10 ns. A detailed description of the experimental setup has been given elsewhere along with basic details of the equipment and its data collection system.[56] Absorbed doses per pulse were on the order of 2−10 Gy (1 Gy = 1 J kg^{-1}). Experiments were performed with a continuous flow of sample solutions at room temperature (~23 °C). Experimental error limits were ± 10% unless specifically noted.

Pulse irradiation of water leads to the formation of the primary reactive species shown in reaction 1:

$$H_2O \wedge\wedge\wedge\wedge \rightarrow {}^{\bullet}OH,\ e^-_{aq},\ {}^{\bullet}H \qquad (1)$$

At pH 5.5, the radiation-chemical yields (G) of $^{\bullet}$OH radicals and e^-_{aq} are equal to G = 0.28 μmol J^{-1}.[57] In N_2O-saturated solutions at pH 5.5, hydrated electrons, e^-_{aq}, are converted into $^{\bullet}$OH radicals (in the presence of H^+) according to reaction 2 (k_2 = 9.1 × 10^9 M^{-1} s^{-1})[58] resulting in a corresponding increased yield of $^{\bullet}$OH radicals:

$$e^-_{aq} + H_2O + N_2O \rightarrow N_2 + {}^{\bullet}OH + HO^- \qquad (2)$$

Therefore, in N_2O-saturated aqueous solutions at pH 5.5, one estimates that the radiation-chemical yields for $^{\bullet}$OH-induced oxidations and H-abstractions should be twice as much as those in N_2-saturated aqueous solutions. The G values for these reactions can be calculated from the Schuler formula (eq 3):

$$G(S^{\bullet}) = 0.539 + 0.307\frac{\sqrt{19.6[S]}}{1 + \sqrt{19.6[S]}} \qquad (3)$$

https://dx.doi.org/10.1021/acs.jpcb.0c04371
J. Phys. Chem. B 2020, 124, 8082−8098

Scheme 1. The First Step of the Mechanism of the •OH-Induced Oxidation of the γ-Glu-(Pro)$_n$-Met Peptides (n = 0−3)

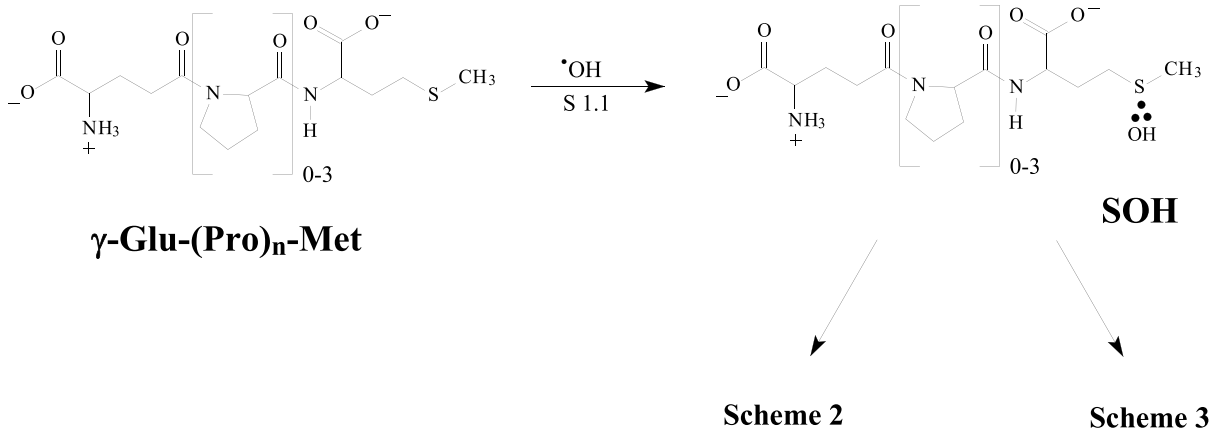

where [S] is the •OH-scavenger concentration.[59] This form of the Schuler formula gives $G(S^{\bullet})$ in units of μmol J^{-1}, and with respect to the current work, [S] = 0.2 mM gives $G(S^{\bullet})$ = 0.557 μmol J^{-1}. The dosimetry was based on N_2O-saturated solutions of 10^{-2} M KSCN, which, following radiolysis, produces $(SCN)_2^{\bullet-}$ radicals that have a molar absorption coefficient of 7580 M^{-1} cm^{-1} at λ = 472 nm and are produced with a yield of G = 0.635 μmol J^{-1} from eq 3.[60]

2.3. Spectral Resolutions of Transient Absorption Spectra. Prior to the determination of radiation-chemical yields, a set of kinetic traces was collected for a sequence of monitoring wavelengths between 260 and 600 nm at 5 nm intervals up to 300 nm and at 10 nm intervals up to 600 nm. For each individual kinetic trace acquired, the data-acquisition systems automatically generate 10 kinetic traces on 10 distinct time scales. This redundancy of time scales makes it relatively easy to assemble transient absorbance spectra at convenient time delays following the pulse of electrons in pulse radiolysis. In order to obtain resolved experimental spectra where the optical density is replaced by the radiation-chemical yield G value, we converted those spectra from OD to $G \times \varepsilon$ using the dosimetry described above.

Based on our previous results with peptides containing Met or S-Me-Glu and N-terminal γ-Glu residues,[36−38,48,49] we can expect the formation of numerous transients with overlapping optical absorption bands. Moreover, two of them, α-(alkylthio)alkyl radicals (αS) and α-aminoalkyl radicals (αN), have similar optical absorption shapes and intensities in the UV region <300 nm. For this reason, the spectral-resolution procedure used earlier by us[61] cannot be applied to resolve these two species to reliably compute their initial radiation-chemical yields. In order to achieve this we applied a slightly modified spectral-resolution procedure consisting of three steps (see Figures S1−S4 in the Supporting Information). Since the radiation-chemical yield of αN radicals ($G_{\alpha N}$) can be measured independently (*vide infra*), their contribution ($G_{\alpha N} \times \varepsilon_{\alpha N}(\lambda_i)$) in the resulting experimental spectra ($G \times \varepsilon(\lambda_i)$) can be easily determined and subtracted from the experimental spectra (step 1 in Figures S1−S4 in the Supporting Information). Subsequently, the spectra resulting from that subtraction, expressed as $(G \times \varepsilon(\lambda_i)) - (G_{\alpha N} \times \varepsilon_{\alpha N}(\lambda_i))$, were decomposed into the component spectra associated with the various transient species present via a multiple linear regression method based on writing the change in $G\varepsilon$:

$$G\varepsilon(\lambda_i) = \sum_j \varepsilon_j(\lambda_i) G_j \quad (4)$$

where ε_j is the molar absorption coefficient of the jth species and the regression parameters, G_j, are equal to the radiation-chemical yield of the jth species (step 2 in Figures S1−S4 in the Supporting Information). The sum in eq 4 is over all species present except for αN radicals. For any particular time delay of an experiment, the regression analysis included equations such as eq 4 for each λ_i under consideration. Thus, the spectral resolutions were made using eq 4 by fitting the reference spectra to the observed transient spectra, transformed from OD(λ) to $G\varepsilon(\lambda)$. The last stage involves re-addition of the contribution of αN radicals to the contributions of radicals obtained from the spectral resolutions based on eq 4 (step 3 in Figures S1−S4 in the Supporting Information).

The reference spectra of these transients (except α-amidoalkyl radicals (αN_{subst})) were previously collected and applied in the spectral resolutions (Figure S5 in the Supporting Information).[40] The molar absorption coefficients of the relevant transients, which will be further identified below, are provided in the following: αS (α-(alkylthio)alkyl radicals, λ_{max} = 290 nm and ε_{290} = 3000 M^{-1} cm^{-1}),[62] αN (α-aminoalkyl radicals, λ_{max} = 265 nm and ε_{265} = 2560 M^{-1} cm^{-1}),[34] $(S\therefore S)^+$ (dimeric intermolecular (S∴S)-bonded radical cations, λ_{max} = 480 nm and ε_{480} = 6880 M^{-1} cm^{-1}),[63,64] and ((S∴O)-bonded radicals, λ_{max} = 390 nm and ε_{390} = 3000 M^{-1} cm^{-1}).[65,66] The S∴OH radicals (OH adduct to the sulfur atom with λ_{max} = 340 nm and ε_{340} = 3400 M^{-1} cm^{-1})[67] were not observed because of their short lifetime except for γ-Glu-(Pro)$_3$-Met.

Since the spectrum of αN_{subst} radicals was not known earlier, we obtained its reference spectrum, characterized by an absorption peak located at λ_{max} = 370 nm, by pulse irradiation of N_2O-saturated aqueous solutions, pH 5.9, containing 10^{-3} M of *N*-ethylacetamide ($H_3C-(C{=}O)-NH-CH_2-CH_3$). There are three possible H-atom abstractions in this molecule, namely, from two methyl groups and one from the *N*-methylene group. Considering that abstraction from the *N*-methyl group of *N*-methylated amides is at least one order of magnitude faster than from the α-methyl group,[68] and taking into account bond dissociation energies of C−H bonds in CH_3 and CH_2 groups (431.6 and 410.6 kJ mol^{-1}, respectively), one can assume that •OH radicals react by hydrogen-atom abstraction almost exclusively from the methylene group. Based on the absorption spectrum (Figure S6 in the Supporting Information), the molar absorption coefficient of

https://dx.doi.org/10.1021/acs.jpcb.0c04371
J. Phys. Chem. B 2020, 124, 8082−8098

Scheme 2. The Mechanism of the •OH-Induced Oxidation of the Met Residue in the γ-Glu-(Pro)$_n$-Met Peptides (n = 0−3) at pH around 5.2−5.5. This Part of the Mechanism Is of Particular Importance for the Discussion of the Main Reaction Pathways and Transient Species of the Peptide with n = 3 Pro Residues

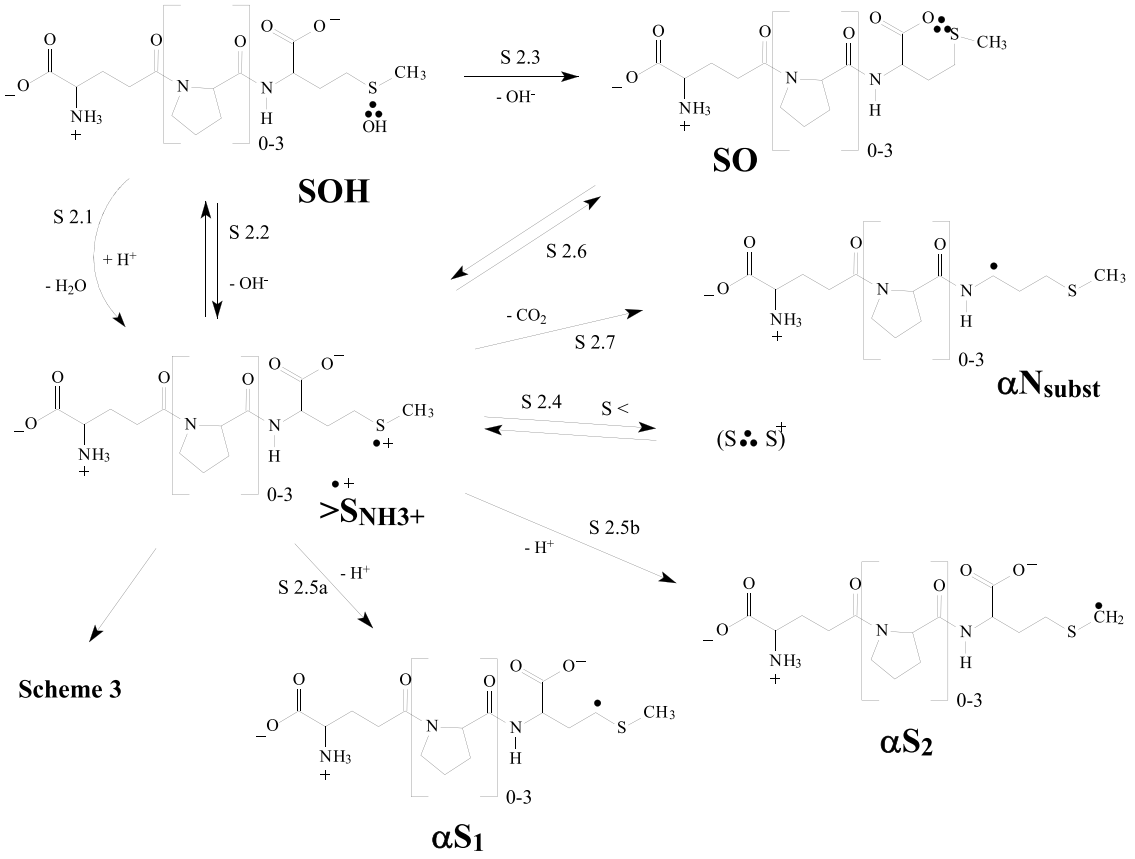

$H_3C-(C{=}O)-NH-CH^{\bullet}-CH_3$ radical at λ_{max} = 370 nm was determined to be equal to ε_{370} = 2000 M^{-1} cm^{-1}.

In all of the experiments, the concentrations of the γ-Glu-(Pro)$_n$-Met substrates were kept sufficiently low so that the formation of intermolecular $(S\therefore S)^+$ was kinetically unfavorable. The intermolecular $(S\therefore S)^+$ radical cation had to be only included into the spectral mix of the derivative with the longest Pro bridge (n = 3).

3. RESULTS AND DISCUSSION

The purpose of these experiments was to understand to what extent peptide-chain dynamics can influence the primary and secondary free-radical reactions of oligopeptides, in particular, γ-Glu-(Pro)$_n$-Met. As mentioned in Section 1, •OH radicals can be used as a radical trigger. In the current study, the triggering reaction was S1.1 in Scheme 1. Previous works on γ-Glu-Met reported that such an SOH product radical from reaction S1.1 can lead to secondary radicals following decarboxylation.[36,48] One of these post-decarboxylation radicals, αN, can be probed by its reaction with p-nitroacetophenone (PNAP) that forms a radical anion of PNAP ($PNAP^{\bullet-}$), see subsection 3.1.3. The yield of $PNAP^{\bullet-}$ was monitored by optical absorption as a function of the proline chain lengths in the different γ-Glu-(Pro)$_n$-Met peptides.

In order to explain the chain-length observations in a quantitative manner, it is necessary to account for the various competing secondary radical reactions. In order to accomplish this, the background radical chemistry is given in Section 3.1. In this section, the established radical reactions from the literature are used to formulate a possible overall mechanism that can account for observed distance dependence of the decarboxylation. This mechanism is presented in Schemes 2 and 3 of Section 3.1. These schemes form a fundamental background assumption for our kinetics analysis in Section 3.3. In the end, the proposed mechanism and the extra kinetics assumptions rise and fall on the overall correspondence of the calculations with the observations.

3.1. •OH-Induced Oxidation: Pulse Radiolysis. The reactions were carried out in N_2O-saturated aqueous solutions, pH 5.2−5.5, containing a 0.2 mM peptide. These experimental conditions were chosen in order to minimize the formation of intermolecularly S∴S-bonded radical cations (reaction S2.4 in Scheme 2) but also to maximize the yields of the other potential intermediates such as αN, αS, αN$_{subst}$, intramolecularly six-membered S∴O-bonded species, and/or intramolecularly five-membered S∴N-bonded species (Schemes 2 and 3).

3.1.1. Absorption Spectra. Transient absorption spectra were recorded in the range of 250 ns to 150 μs after the electron pulse (see Figure 1) in N_2O-saturated solutions containing γ-Glu-(Pro)$_n$-Met (n = 0−3). At short delay times, these spectra showed a dominant broad absorption band with a distinct λ_{max} around 280−290 nm and a weakly pronounced band at λ_{max} around 370−380 nm. The 370−380 nm band became increasingly visible as the number of Pro residues increased (Figure 1C,D). These spectral observations are a strong indication (i) that α-(alkylthio)alkyl radicals (αS) and/or α-aminoalkyl radicals (αN) were present in the dominant

https://dx.doi.org/10.1021/acs.jpcb.0c04371
J. Phys. Chem. B 2020, 124, 8082−8098

Scheme 3. The Mechanism of the •OH-Induced Oxidation of the Met Residue in the γ-Glu-(Pro)$_n$-Met Peptides (n = 0−3) at pH around 5.2−5.5. This Part of the Mechanism is of Particular Importance for the Discussion of the Main Reaction Pathways and Transient Species of the Peptide with n = 0−2 Pro Residues

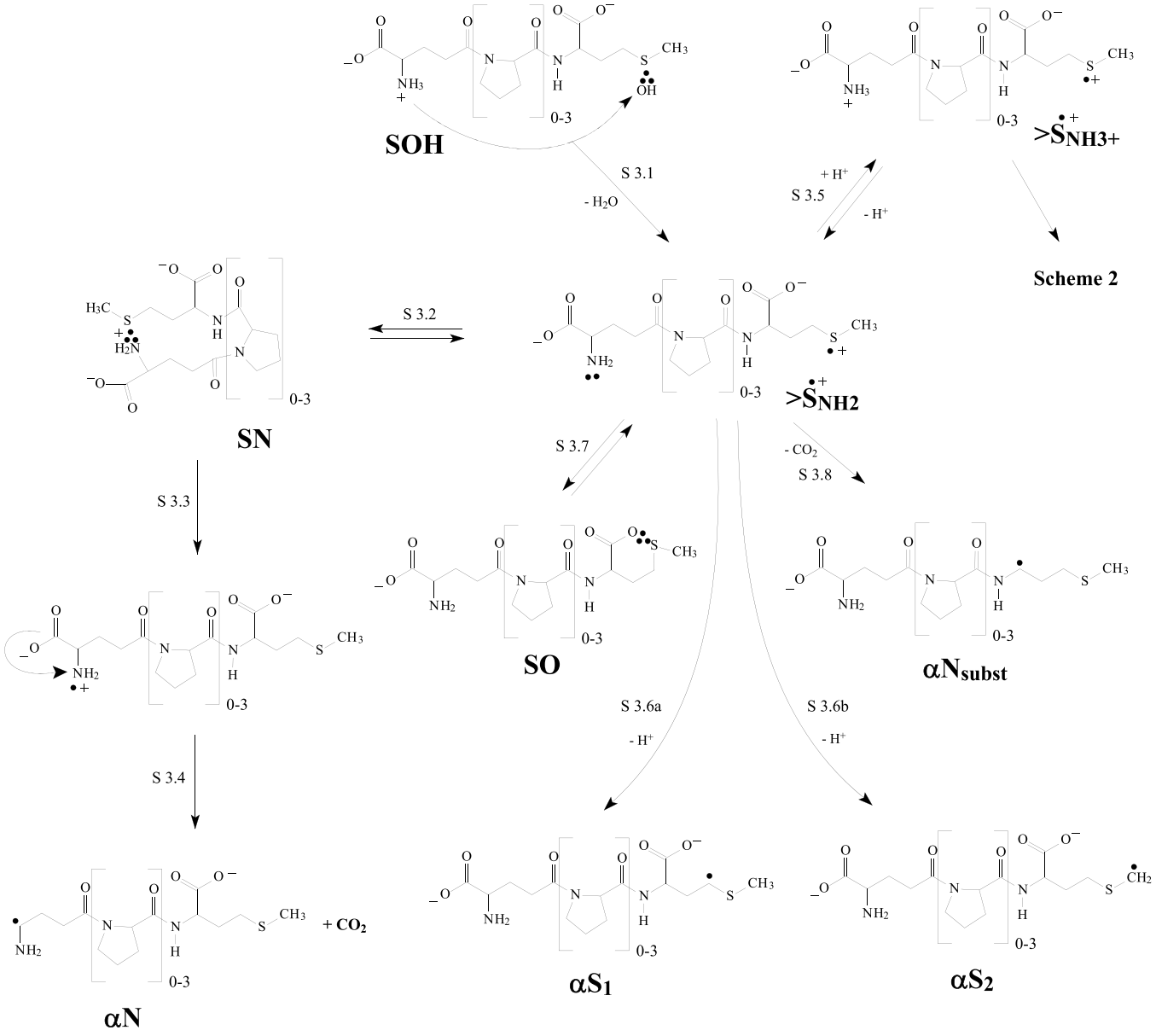

absorption band (280−290 nm) and (ii) that (S∴O)-bonded radicals or (S∴N)-bonded radicals and/or αN_{subst} radicals were present in the weakly pronounced, longer-wavelength band (370−380 nm). Interestingly, transient absorption spectra from γ-Glu-(Pro)$_3$-Met showed the development of a shoulder at λ = 490−510 nm in the time domain of 600 ns to 7 μs. This spectral feature is assigned to an intermolecularly formed (S∴S)-bonded radical cation (Figure 1D). The spectral resolutions below support this assignment. Insets in all four parts of Figure 1 show kinetic traces for the growth of α-amino type radicals (αN) and, to a lesser extent, the growth of α-(alkylthio)alkyl radicals (αS) observed at 265 nm. These kinetic traces look very similar, and they reached their maximum signal after approximately 4 μs.

3.1.2. Mechanism for the •OH-Induced Oxidation: Potential Transients. This subsection has a dual role. Its first role is to familiarize the reader with the appropriate scientific background on the chemistry of sulfur radicals in peptides. Its second role is to provide arguments based on kinetic and spectral analyses from the literature for the presence of potential transients. This is a key issue that enables our resolution of the experimental absorption spectra of numerous transients with overlapping optical absorption bands as well as providing justification for the mechanistic assumptions used in the kinetics analysis below in Section 3.3.

Formation of an •OH adduct to the sulfur moieties in the C-terminal Met residues in the form of three-electron-bonded transients Met(S∴OH) has been established as the first step in the •OH-induced oxidation of the peptides containing the Met residue (reaction S1.1) in Scheme 1.[63,69]

The SOH radical has been shown to decay along four different pathways presented in Schemes 2 and 3: (i) by using protons from the bulk of the solution (reaction S2.1), (ii) by spontaneous dissociation (reaction S2.2), (iii) by intra-

https://dx.doi.org/10.1021/acs.jpcb.0c04371
J. Phys. Chem. B 2020, 124, 8082−8098

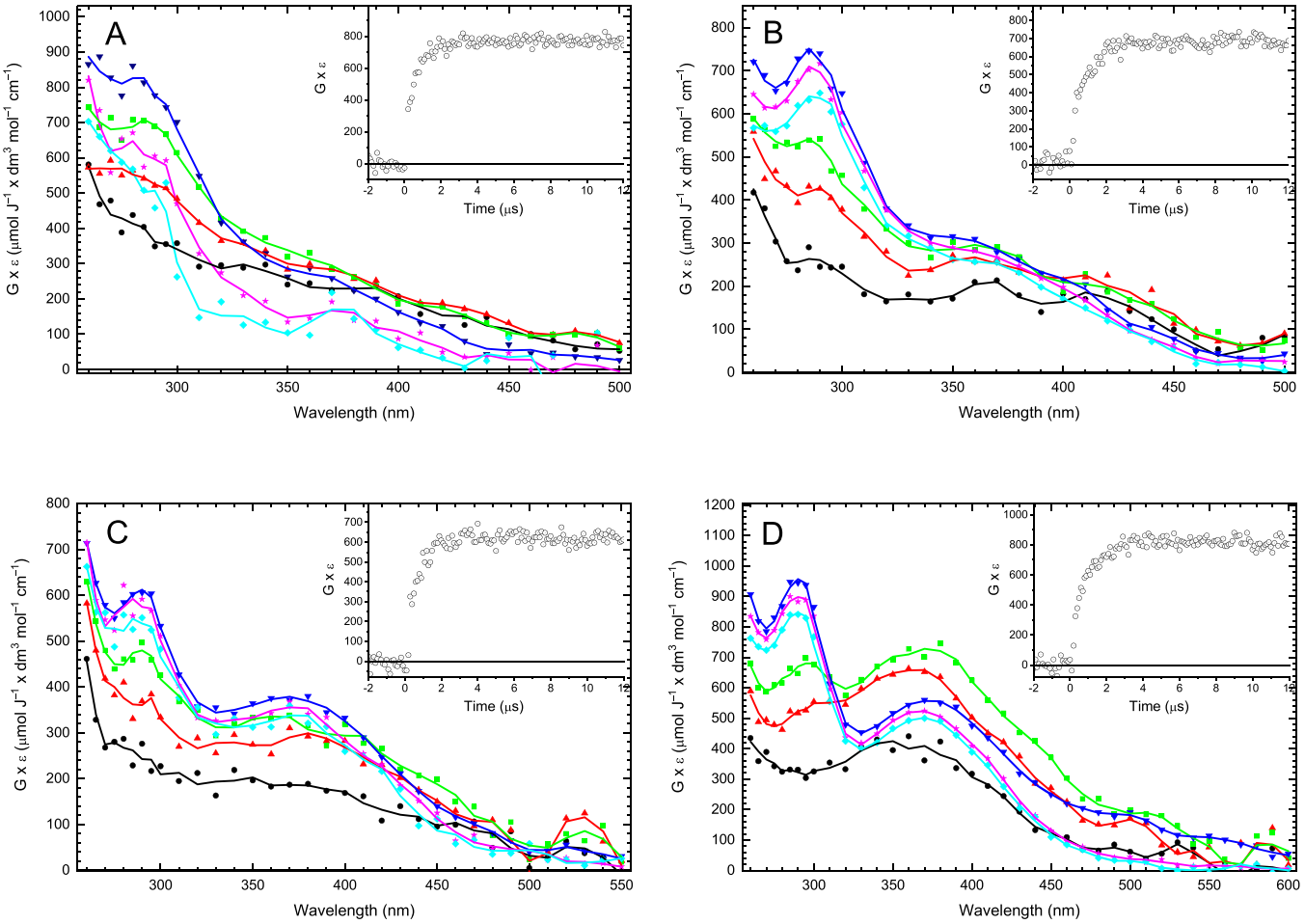

Figure 1. Evolution of the transient absorption spectra following $^{\bullet}$OH-induced oxidation of (A) γ-Glu-Met (0.2 mM), (B) γ-Glu-Pro-Met (0.2 mM), (C) γ-Glu-Pro$_2$-Met (0.2 mM), and (D) γ-Glu-Pro$_3$-Met (0.2 mM) in N_2O-saturated aqueous solutions, pH = 5.2−5.5. Spectra recorded after different time delays after the electron pulse: (black circles) 250 ns, (red up triangles) 600 ns, (green squares) 1 μs, (blue down triangles) 8 μs (A), 11 μs (B), 7 μs (C and D), (purple stars) 50 μs, (cyan diamonds) 100 μs. Insets: Kinetics traces for the growth of a radical formation observed at λ = 265 nm.

molecular carboxylate-assisted elimination of OH^- and formation of the (S∴O)-bonded radical (reaction S2.3), and (iv) by using the proton from a terminal NH_3^+ (reaction S3.1).

Some idea of the contributions of SOH to the $^{\bullet}$OH-triggered reactions can be obtained by focusing only on the 340 nm kinetic traces of the transient spectra in Figure 1 (340 nm is the spectral maximum of SOH radicals). These 340 nm kinetic traces are shown in Figure 2. The known lifetimes of SOH radicals are several microseconds or less. So, the kinetic traces for peptides with n = 1−2 are too long-lived to be assigned to SOH radicals, which indicates that SOH radicals for these three compounds were much too short-lived and not observed on this time scale. In particular, the SOH radicals in these three compounds were formed rapidly and decayed as their successor radicals were formed. On the other hand, the trace for n = 3 is consistent with SOH radicals, and we assign the short-lived component to the SOH radical of the peptide with n = 3.

Even though the overall lifetimes of the SOH radicals from n = 0−2 were too short to be observed in Figures 1 and 2, the individual, underlying, primary decay rate constants for all four of the SOH radicals can still be estimated. The decay trace of SOH radical for n = 3 will be used below to calibrate these calculations. The basis for this approach is that the local

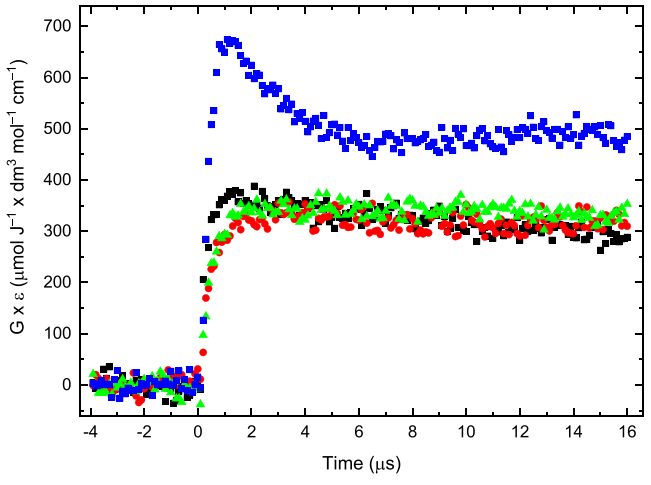

Figure 2. Kinetic traces for the growth and decay of radicals observed at λ = 340 nm in N_2O-saturated aqueous solutions, pH = 5.2−5.5, containing 0.2 mM γ-Glu-(Pro)$_n$-Met peptides: n = 0 (black squares), n = 1 (red circles), n = 2 (green triangles), and n = 3 (blue squares).

neighborhoods of the SOH sites are similar in all four SOH radicals. In particular, this assumption applies to reactions S2.1, S2.2, and S2.3. Only reaction pathway S3.1 could vary because

https://dx.doi.org/10.1021/acs.jpcb.0c04371
J. Phys. Chem. B 2020, 124, 8082−8098

of variation in end-to-end distances between the four SOH radicals. The motivation for making these calculations is to determine the extent to which intramolecular proton transfer S3.1 competes with the other three decay channels of SOH, i.e., S2.1, S2.2, and S2.3. The extent to which S3.1 occurred will be central to rationalizing the experimental observations based on the above schemes.

Taking the first reaction S2.1 for the reaction of SOH radicals with external protons, its rate constant can be estimated from the following literature and calculation. The second-order rate constant ($k_{S2.1}$) for the reaction of SOH radicals with protons was reported to be 1.1×10^{10} M^{-1} s^{-1} for *N*-acetylmethionine.[70] Taking this value as typical for the four SOH radicals, we calculated that the half-life of SOH radicals under our conditions (pH = 5.5 and low dose) would be ∼28 μs assuming that the SOH radicals were decaying only via reaction pathway S2.1 (see Comment S1 in the Supporting Information).

The second primary decay channel of SOH radicals, S2.2, can be estimated taking the first-order rate constant for the spontaneous dissociation ($k_{S2.2}$) as 6.3×10^5 s^{-1} (estimated for *N*-acetylmethionine).[70] If the SOH radicals were decaying only via reaction pathway S2.2, then its half-life would be ∼1.1 μs. Based on kinetics taken at λ = 340 nm (Figure 2), we can see that the half-lives of SOH radicals were all much shorter than 1.1 μs except for γ-Glu-$(Pro)_3$-Met whose fitted half-life was almost the same as that for the spontaneous dissociation of (S∴OH) from *N*-acetylmethionine.

In regard to process S2.3, earlier simulations using Langevin Dynamics for Thr-$(Pro)_n$-Met peptides showed that the mean distances between carboxylate carbon atoms and the sulfur atom in the C-terminal Met residue in Met(S∴OH) radical varied only slightly with the expansion of the N-terminal peptide sequence to Met.[35] Therefore, the intramolecular carboxylate-assisted decay of SOH radical (reaction S2.3) should occur with similar rate constants ($k_{S2.3}$) for all of the γ-Glu-$(Pro)_n$-Met peptides studied. Again, this is further justification for the local environments of the SOH site being similar for all four radicals in γ-Glu-$(Pro)_n$-Met peptides (n = 0−3).

Some limits can be put on the magnitude of rate constants ($k_{S2.3}$). Relevant evidence can be found in the literature and in comparison to the estimates above for the rate constants of decay processes (S2.1) and (S2.2). Studies on the rate constants $k_{S2.3}$ for reaction S2.3 as high as 10^7−10^8 s^{-1} were reported in regard to five-membered S∴O-bonded rings in thiopropionic acids.[71] However, this range should be considered only as an upper limit to the six-membered (S∴O)-bonded rings that would be possible for the peptides in the current study because the formation of five-membered structures of intramolecularly (S∴O)-bonded radicals is kinetically preferred over six-membered structures. Particularly relevant evidence for this contrast between formation rates of five- vs six-membered (S∴O)-bonded rings was presented where such five-membered rings were observed in 3-(methylthio)propanol, but no such six-membered rings were observed in 4-(methylthio)butanol.[65] More concrete estimates for $k_{S2.3}$ can be made with the following conjectures based on the data presented in Figure 2. If the short-lived component of the kinetic trace in γ-Glu-$(Pro)_3$-Met at λ = 340 nm is assigned to the SOH radical, then the estimated upper limit for formation of (S∴O)-bonded radicals (based on the thiopropionic acids) cannot be attained. If the (S∴O)-bonded radicals were formed so rapidly, then the SOH radical could not live long enough to be observed as it is in the kinetic trace for γ-Glu-$(Pro)_3$-Met in Figure 2. Since it has already been concluded above that the formation rates of (S∴O)-bonded radicals in this study are likely to be similar, it can be concluded that the (S∴O)-bonded ring formation is also so limited in all four compounds under study. Moreover, this argument can be taken another step to limit the rate of (S∴O)-bonded ring formation even further. Referring again to the similar half-lives of the (S∴OH) radical of *N*-acetylmethionine and the half-life of the analogous species in γ-Glu-$(Pro)_3$-Met in Figure 2, the intramolecular carboxylate-assisted decay of SOH radical cannot occur with the rate constant higher or even equal to the rate constant for its spontaneous dissociation, i.e., $k_{S2.2}$. Otherwise, the lifetime of the SOH radical in the γ-Glu-$(Pro)_3$-Met peptide would be shorter than that observed in Figure 2.

Based on the above estimates for the decay rate constants for competing SOH radical decay rate constants of S2.1, S2.2, and S2.3, the rate constant for the distance-dependent intramolecular proton-transfer reaction from N-terminal NH_3^+ (S3.1) would be much higher than that for reactions (S2.2) and (S2.3) for γ-Glu-$(Pro)_n$-Met peptides with n = 0−2 (see estimates in Section 3.3 and Comment S2 in the Supporting Information). On the other hand, for γ-Glu-$(Pro)_3$-Met, the rate constant of intramolecular proton transfer reaction ($k_{S3.1}$) would be lower than $k_{S2.2}$.

Schemes 2 and 3 illustrate also the different ways that the monomeric sulfur-centered radical cations Met(>$S^{\bullet+}$) can decay. However, if Met(>$S^{\bullet+}$) were to be formed with the proton from the N-terminal amino group transferring intramolecularly to the >S∴OH moiety located on the C-terminal Met residue (S3.1), then this resulting Met(>$S^{\bullet+}$) would be formed in the peptide molecule with an unprotonated amino group (>$S^{\bullet+}{}_{NH2}$). In the range of pH studied (5.2−5.5), only for a very short time (computed in Comment S3 in the Supporting Information) would the oxidized peptide molecule contain the unprotonated amino group, which would allow for the formation of the very short-lived S∴N-bonded radical cation (S3.2). Such an S∴N-bonded radical cation can be a precursor of reducing αN radicals formed via consecutive reactions S3.3 and S3.4. Any yields of such αN radicals can be easily probed by *p*-nitroacetophenone (PNAP) (*vide infra*).

Regardless of the protonation status of the amino group in the oxidized peptide molecule, any oxidized peptide molecule, still containing Met(>$S^{\bullet+}$), can undergo several competitive reactions. The first two are common to thioethers in general.[72] The first reaction pathway for Met(>$S^{\bullet+}$) would be to form intermolecularly (S∴S)-bonded radical cations (S2.4). The second pathway would involve two different deprotonations both producing αS radicals (S2.5a and S2.5b in >$S^{\bullet+}{}_{NH3+}$) and (S3.6a and 3.6b in >$S^{\bullet+}{}_{NH2}$). (>$S^{\bullet+}{}_{NH3+}$ is the notation for >$S^{\bullet+}{}_{NH2}$ with its amino group protonated.)

When the thioethers contain functional substituents, there are other possible reaction pathways involving intramolecular neighboring-group effects.[73,74] In the case of the peptides studied, the neighboring-group effects apply to nitrogen and oxygen atoms in peptide bonds and oxygen atoms in carboxyl groups, which can provide a lone pair of electrons to bond with the monomeric sulfur cation (>$S^{\bullet+}$) forming 2*c*-3*e* S∴N and S∴O-bonds, respectively. The first kind of interactions can be excluded for Coulombic reasons. Owing to resonance (eq 5) with the neighboring carbonyl group, the N-atom should carry

https://dx.doi.org/10.1021/acs.jpcb.0c04371
J. Phys. Chem. B 2020, 124, 8082−8098

a positive charge and thus prevent efficient approach of $>S^{\bullet+}$ to the $=NH^{+}-$ moiety in the oxidized peptides:[48]

$$\sim -C(=O)-NH-CH(CH_2CH_2SCH_3)-COO^- \leftrightarrow \sim -C(-O^-)=NH^+-CH(CH_2CH_2SCH_3)-COO^- \quad (5)$$

Taking these considerations together, one can conclude that cyclic five-membered $S.\therefore NH^+$ radical cation formed at the C-terminal should not be considered in the spectral-resolution analyses.

On the other hand, a cyclic six-membered $S.\therefore O$ radical can be formed at the C-terminus in the next pathway of disappearance of monomeric sulfur-centered radical cations Met($>S^{\bullet+}$). This species can lead to the reconstruction of Met($>S^{\bullet+}$) in a reversible cyclization reaction (S.2.6 in $>S^{\bullet+}{}_{NH3+}$ and S3.7 in $>S^{\bullet+}{}_{NH2}$). A similar species was observed during the one-electron oxidation of Thr-Met by sulfate radical anions ($SO_4^{\bullet-}$) in aqueous solutions.[34]

Finally, Met($>S^{\bullet+}$) can also potentially decay via an intramolecular electron transfer with the C-terminal carboxylate group (pseudo-Kolbe mechanism) that would generate an α-amidoalkyl radical (αN_{subst}) (S2.7 in $>S^{\bullet+}{}_{NH3+}$ and S3.8 in $>S^{\bullet+}{}_{NH2}$).[48] These particular αN_{subst} radicals cannot be probed by the formation of the PNAP radical anion ($PNAP^{\bullet-}$) due to their weaker reducing properties compared to αN radicals. This was experimentally confirmed by a comparison between $G(CO_2)$ and $G(PNAP^{\bullet-})$ measured after $^{\bullet}OH$-induced oxidation of γ-Glu-Met and *S*-methylglutathione[36] and by the comparison of $G(MV^{\bullet+})$ measured after $^{\bullet}OH$-induced decarboxylation of methionine and *N*-acetylmethionine, which led to αN and αN_{subst} radicals, respectively.[75] Moreover, based on the experimental fact that αN radicals derived from Met were able to reduce nicotinamide adenine dinucleotide (NAD^+), their reduction potential must be more negative than −0.94 V (E^0 vs NHE).[75] Furthermore, the quantum-chemical calculations clearly showed that αN radicals are stronger reductants than αN_{subst} radicals (E^0 vs NHE: −0.66 V vs +0.36 V, respectively), showing that αN_{subst} radicals are rather oxidants not reductants.[76]

Since it was not possible to follow the transients directly from the raw data because of the significant overlap of their absorption spectra, the experimental spectra recorded at different times after the pulse (Figure 1) were resolved into contributions from the following five components: αN, αN_{subst}, αS, SO, and $(S.\therefore S)^+$ radicals (see their structures in Schemes 2 and 3). SOH radicals (see their structure in Scheme 1−3) were not included in the spectral mix of the spectral resolutions because of their very short lifetime (<0.5 μs), except for the peptide with three Pro residues (≈1 μs) (see kinetics at 340 nm in Figure 2) at pH 5.5. Two of the species (αN and αS radicals) were distinguished by their redox properties since αN is a stronger reductant than αS and was able to selectively reduce PNAP. No reduction potential has been reported for αS radicals formed in Met residues. However, it was shown that the αS radicals formed exclusively after decarboxylation of 2,2′-thiodiethanoic acid were not able to reduce PNAP to $PNAP^{\bullet-}$.[77] Therefore, their reduction potential must be less negative than −0.36 V, which corresponds to E^0 vs NHE for $PNAP/PNAP^{\bullet-}$.[78]

3.1.3. Independent Determination of the Radiation-Chemical Yields of α-Aminoalkyl Radicals (αN). It has been shown that *G* values for the formation of C-centered, α-aminoalkyl (αN) radicals obtained from the N-terminal decarboxylation reaction (Scheme 3) can be measured either by their direct observation or by probing via their reaction with *p*-nitroacetophenone (PNAP) (see eq 6).[36,37] The latter procedure leads to a $PNAP^{\bullet-}$ radical anion (with a molar absorption coefficient ε_{360} = 17,600 M^{-1} cm^{-1}).[79]

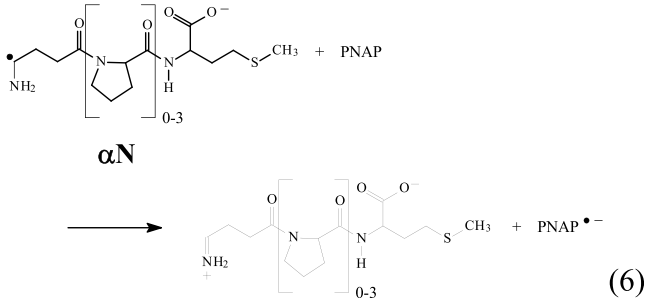

(6)

The formation of $PNAP^{\bullet-}$ radical anions in the reaction presented in eq 6 was investigated in N_2O-saturated aqueous solutions containing γ-Glu-$(Pro)_n$-Met (n = 0−3) peptides and PNAP at the concentrations of 0.2 and 0.03 mM, respectively, at pH 5.4 (Figure 3). These experimental conditions were chosen in order to minimize the reaction of $^{\bullet}OH$ radicals with PNAP and the direct reduction of PNAP by hydrated electrons.

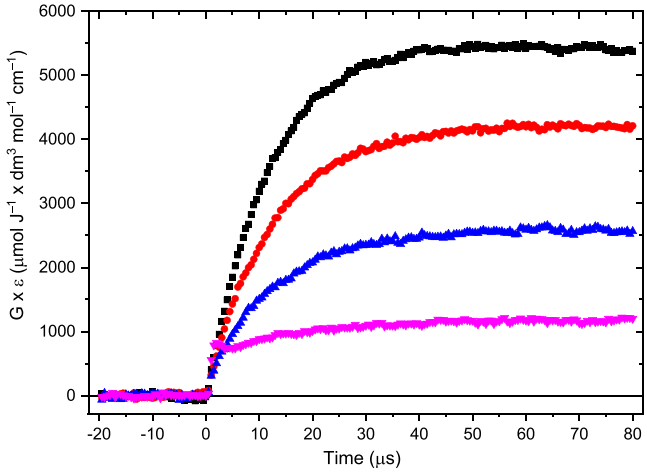

Figure 3. Kinetics of PNAP radical anion formation (taken at 360 nm) after $^{\bullet}OH$-induced oxidation of γ-Glu-$(Pro)_n$-Met (0.2 mM) (n = 0−3) by PNAP (*p*-nitroacetophenone) (3 × 10^{-5} M) in N_2O-saturated aqueous solutions, pH ≈ 5.4: (black squares) n = 0, (red circles) n = 1, (blue up triangles) n = 2, and (pink down triangles) n = 3.

All of these kinetic traces in Figure 3 were corrected for the background radical absorption at 360 nm. Appropriate values of $G(PNAP^{\bullet-})$, determined from the respective plateau values of corrected kinetic traces (Figure S7 in the Supporting Information) and taken as $G(\alpha N)$ are listed in Table 1.

3.1.4. Potential Contribution of Radicals Derived from Pro Residues. Another issue, which had to be clarified before any resolutions of the spectral components were performed, was

https://dx.doi.org/10.1021/acs.jpcb.0c04371
J. Phys. Chem. B 2020, 124, 8082−8098

Table 1. Radiation-Chemical Yields (G) of Transients Formed after $^{\bullet}$OH-Induced Oxidation of γ-Glu-$(Pro)_n$-Met Peptides (n = 0−3)

G from Pulse Radiolysis (μmol/J)[a, b]					
Peptide	$PNAP^{\bullet-}$ [c] (αN)	αN_{subst}	αS	SO	SS^{+}
γ-Glu-Met	0.31	0.05	0.03	0.03	0
γ-Glu-$(Pro)_1$-Met	0.22	0.06	0.07	0.04	0
γ-Glu-$(Pro)_2$-Met	0.13	0.07	0.09	0.07	0
γ-Glu-$(Pro)_3$-Met	0.04	0.11	0.26	0.10	0.01

[a] G values of radicals were calculated within ∼20% error, about 7−11 μs after the electron pulse, which corresponded to the maximum concentration of αN for γ-Glu-$(Pro)_n$-Met peptides. [b] G values were measured at 7−11 μs after the pulse and cannot be extrapolated to t = 0. At 7−11 μs, after the pulse, a fraction of radicals will have reacted via radical-radical reactions, and therefore, the total yield of radicals at 7−11 μs would have been less than the initial yield of $^{\bullet}$OH radicals. The rate constants for the reactions between the individual radicals vary with the type of radical; hence, the loss of radicals via radical-radical reactions will vary between the peptides as the G values for the individual radicals changed with peptide structure. [c] The G values of $PNAP^{\bullet-}$ calculated after correction for the background radical absorption at 360 nm.

whether there were any potential contributions of $Pro^{\bullet}$ radicals potentially being formed by the hydrogen abstraction from C−H bonds by $^{\bullet}$OH radicals from Pro.[80] Taking the respective rate constants for the reaction of $^{\bullet}$OH radicals with Pro, Met, and Glu as 4.8×10^8, 2.2×10^{10}, and 2.3×10^8 M^{-1} s^{-1},[58] it was easy to calculate that the largest contribution of $Pro^{\bullet}$ radicals expected in the peptides would be for the reaction of $^{\bullet}$OH radicals with γ-Glu-$(Pro)_3$-Met and that such a yield would not exceed 6% of the total yield of $^{\bullet}$OH radicals.

3.2. Resolution of the Spectral Components in the Absorption Spectra following $^{\bullet}$OH-Induced Oxidation. Resolutions of absorption spectra (Figure 4) at any desired time delay following the electron pulse were performed using a modified spectral-resolution procedure (*vide supra* in Section 2.3) in order to extract the radiation-chemical yields (G values) for the formation of the intermediates mentioned above.

The G values measured at the given times after the electron pulse, when αN radicals reached their maximum concentration, are listed in Table 1.

3.3. Interactions between an N-Terminal Amino Group and a Side Chain of C-Terminal Methionine Residue by Probing the Distance Dependence between the Nitrogen and Sulfur Atoms on the Yield of α-Aminoalkyl Radicals. Radiation-chemical yields (G) obtained for the formation of αN radicals measured by the complementary formation of $PNAP^{\bullet-}$ radical anions (Table 1) showed a general trend of a decrease in G values with an increase in the number (n) of the Pro residues. These αN radicals were formed in several stages (Scheme 3; S3.2−S3.4). One of them was the formation of a short-lived SN species (Scheme 3, reaction S3.2). This reaction is a distance-dependent cyclization reaction whose yield would have depended on the distance between the N-terminal amino group on the Glu residue and the sulfur atom present in the C-terminal methionine side chain. The obtained radiation-chemical yields of αN radical formation proved that the efficiency of this reaction decreases with the extension of the proline-chain length. On the other hand, radiation-chemical yields for the formation of α-amidoalkyl radicals (αN_{subst}), α-(alkylthio)alkyl radicals (αS), and (S.∴O)-bonded six-membered radical cations (long-lived) at the C-terminal tended to increase with increasing length of the proline bridges (Table 1). We also identified the formation of intermolecular (S.∴S)-bonded radical cations but only for n = 3.

In order to determine a general tendency, the respective G values of transients obtained from pulse radiolysis were plotted against the number of proline residues (Figure 5).

3.3.1. Intramolecular Proton Transfer from the N-Terminal Amino Group to the >S.∴OH Moiety. As discussed in Section 3.1, reaction S3.1 would be a distance-dependent intramolecular proton-transfer reaction to eliminate H_2O, and it has been shown to form the monomeric sulfur-centered radical cation $>S^{\bullet+}$ with unprotonated amino groups ($>S^{\bullet+}{}_{NH2}$). Reactions S2.1 and S2.2 have been shown to form monomeric sulfur-centered radical cations Met ($>S^{\bullet+}$) via the elimination of OH^-, but most importantly, their N-terminal amino groups remain protonated ($>S^{\bullet+}{}_{NH3+}$) in these two reactions. In the formation of cyclic (S.∴O)-bonded six-membered radical cations (S2.3), the resulting oxidized peptides still have their N-terminal amino groups protonated. Such species cannot be precursors of α-aminoalkyl radicals (αN).

At this point, it has to be stressed that a direct contact between the >S.∴OH moiety and the N-terminal protonated amino group does not seem to be necessary because proton-catalyzed elimination of OH^- may involve a shortcut for proton transfer via hydrogen bonds between water molecules in a "proton shuttling" mechanism.[81,82] For this reason, a definite statement whether and how the rate constant for this process depends on the number (n) of proline residues is not entirely possible. The measured half-life (∼1.1 μs, *vide supra*) of the SOH radical of the γ-Glu-Pro_3-Met peptide (Figure 2) fits very well with the expected first-order rate constant for its spontaneous dissociation as 6.3×10^5 s^{-1} (S2.2).[70] In other words, the spontaneous dissociation seems to be in this case the fastest process controlling the lifetime of the SOH radical. Thus, for this peptide with n = 3, spontaneous dissociation represents the main competitive pathway against the intramolecular proton transfer from the amino group to the >S.∴OH moiety (S3.1). In contrast, for the other three peptides, the SOH radicals were not observed despite the fact that, under our experimental conditions (0.2 mM), SOH radicals should have been formed with a rate of 2.4×10^6 s^{-1}. This suggests that other processes controlled the lifetime of the SOH radicals. The two processes (S2.1 and S2.3) can be excluded for the reasons mentioned in Section 3.1. The obvious conclusion imposed at this point is that the lifetimes of the SOH radicals in γ-Glu-Met, γ-Glu-Pro-Met, and γ-Glu-$(Pro)_2$-Met were controlled by the respective rate constants of intramolecular proton transfer (S3.1). Unfortunately, it is not possible to determine these rate constants separately for each of these three peptides and to confirm whether or not there is a general decreasing trend with increasing number of the proline residues from 0 to 2.

https://dx.doi.org/10.1021/acs.jpcb.0c04371
J. Phys. Chem. B 2020, 124, 8082−8098

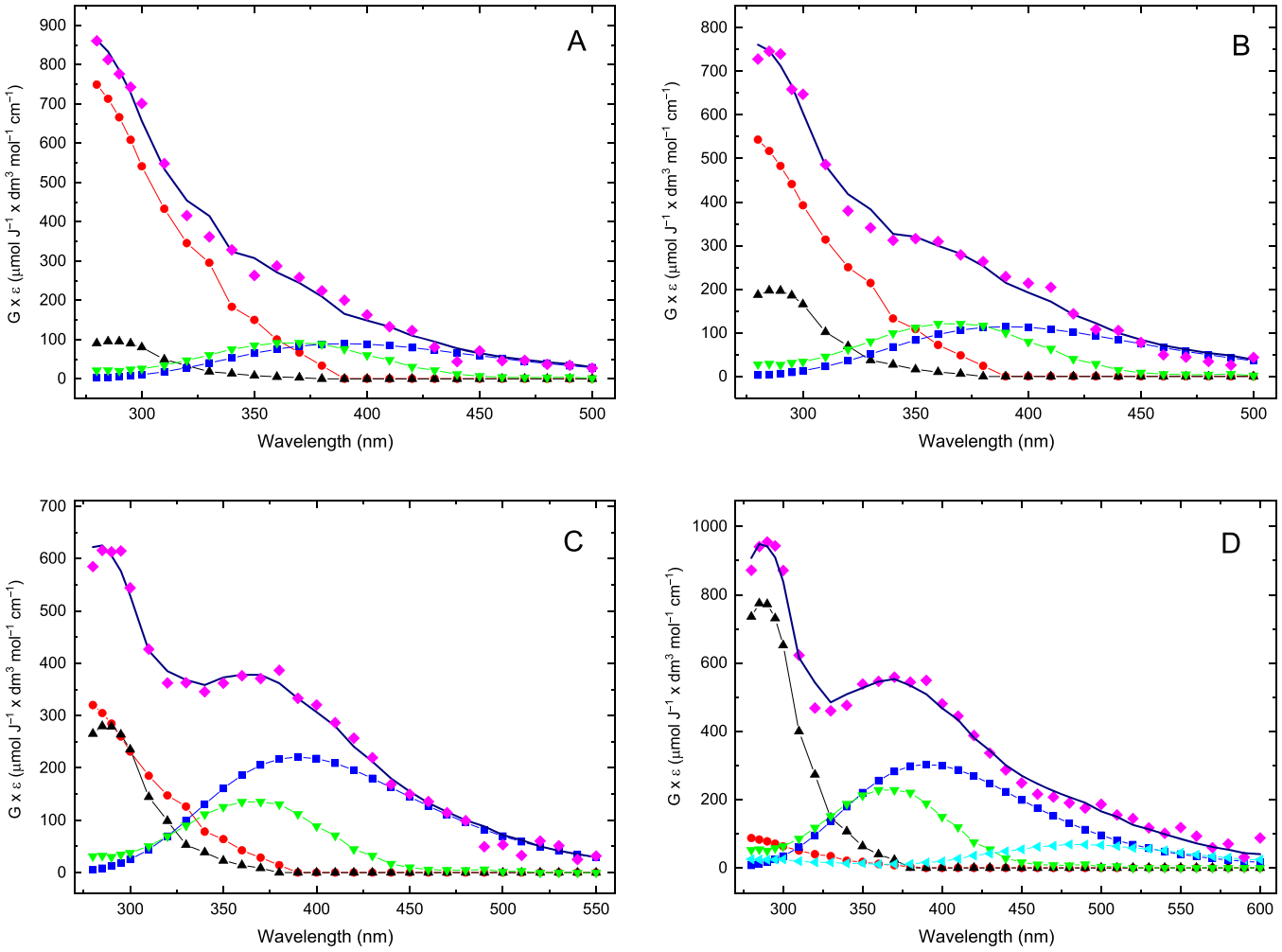

Figure 4. Resolution of the spectral components: αN (red circles), αN_{subst} (green down triangles), αS (black up triangles), SO (blue squares), SS^+ (cyan left-pointing triangles) in the transient absorption spectra (265−600 nm) (experimental (pink diamonds) and fit (solid lines)) recorded 8 μs (A), 11 μs (B), and 7 μs (C, D) after electron pulse following $^{\bullet}$OH-induced oxidation of (A) γ-Glu-Met (0.2 mM), (B) γ-Glu-Pro-Met (0.2 mM), (C) γ-Glu-Pro_2-Met (0.2 mM), and (D) γ-Glu-Pro_3-Met (0.2 mM) in N_2O-saturated aqueous solutions, pH = 5.3−5.6.

It was possible to estimate its lower limit in the γ-Glu-$(Pro)_3$-Met peptide in which the rate of S3.1 has to be definitely lower than 6.3×10^5 s^{-1}. However, for the other three peptides, no SOH radicals were observed. Simulations (see Comment S2 in the Supporting Information) from a simple kinetics model for competitive decay of SOH via two reactions S3.1 and S2.2 (with $k = 6.3 \times 10^5$ s^{-1}) clearly shows that, for the peptides with 0−2 proline residues, the rate of reaction S3.1 has to be much larger than for reaction S2.2 in order for there to be no SOH observed. Thus, as long as there is no observed SOH, an increasing number of Pro residues should not affect significantly the yields of the $>S^{\bullet+}{}_{NH2}$ radical cations formed via reaction S3.1. Based on the known radical chemistry coming out of these particular peptides, these radicals are the only likely precursors of αN radicals. In other words, intramolecular proton transfer (S3.1) from the N-terminal amino group to the >S∴OH moiety, though distance-dependent, cannot be responsible for the observed tendencies in the G values of transients with the increasing number (n) of the Pro residues from 0 to 2 (Figure 5). For these peptides, regardless of the number of Pro residues, none of the other processes that the SOH radical may undergo (S2.1, S2.2, and S2.3), can effectively compete with intramolecular proton transfer from the N-terminal amino group to the >S∴OH moiety (S3.1). So, in principle, the branching ratio of the SOH radicals decaying via intramolecular proton transfer is close to one in the γ-Glu-$(Pro)_n$-Met peptides with n = 0−2. Almost all of the SOH radicals formed in these three compounds decay via intramolecular proton transfer.

3.3.2. Cyclization Reaction Forming (S∴N)-Bonded Multimembered Radical Cations. The second reaction expected to be distance-dependent was a cyclization reaction involving the $>S^{\bullet+}{}_{NH2}$ radical cations forming (S∴N)-bonded multi-membered radical cations (N-terminal) (S3.2). These cyclic radicals are expected to be consecutive precursors of αN-radicals (*vide* S3.3 and S3.4). Such an (S∴N)-bonded multi-membered radical cation can only be formed by direct contact (van der Waals contact) of the $>S^{\bullet+}{}_{NH2}$ radical cation moiety with the deprotonated N-terminal amino group. That amino group would contribute its lone electron pair with the unpaired electron on the $>S^{\bullet+}{}_{NH2}$ moiety to form a 2*c*-3*e* S∴N-bond (S3.2).

3.3.3. Kinetics of Cyclization Reaction and Decarboxylation when n = 0 to 2. The significance of this cyclization and subsequent decarboxylation can be estimated by considering the competition of alternate decay pathways of

https://dx.doi.org/10.1021/acs.jpcb.0c04371
J. Phys. Chem. B 2020, 124, 8082−8098

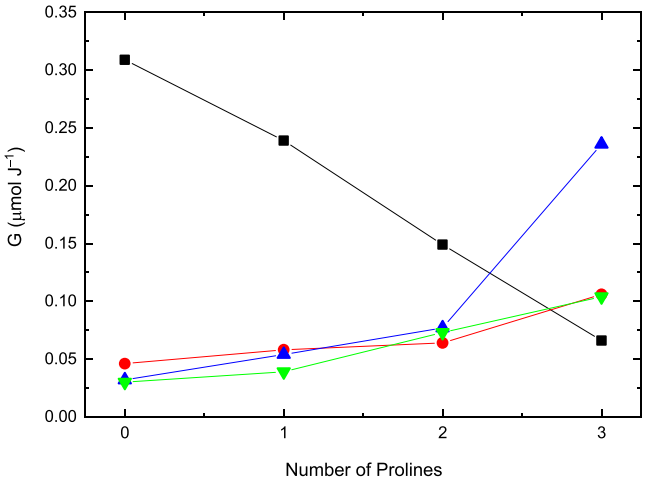

Figure 5. Dependence of radiation-chemical yields (G) of α-aminoalkyl radicals (αN) (black squares), α-amidoalkyl radicals (αN_{subst}) (red circles), α-(alkylthio)alkyl radicals (αS) (blue up triangles), and SO radicals (green down triangles) on the number (n) of proline residues in the case of $^{\bullet}$OH-induced oxidation of γ-Glu-Pro$_n$-Met peptides (0.2 mM) (n = 0−3) in N_2O-saturated aqueous solutions, pH around 5.4.

the $>S^{\bullet+}{}_{NH2}$ radical cation. As argued in the preceding section, when n = 0 to 2, the branching ratio is approximately equal to one for the decay of SOH radicals via water elimination following intramolecular proton transfer (S3.1). Almost all of the SOH radicals' decay then results in $>S^{\bullet+}{}_{NH2}$ radicals with a sulfur radical cationic site and a deprotonated amino group in the N-terminal Glu group. From the enumeration of the competitive reaction pathways starting with this sulfur radical, it is possible to come to some conclusions about the effects of the Pro chain lengths on the reaction yields.

Starting with this $>S^{\bullet+}{}_{NH2}$ radical, the reaction of most interest for this work is the cyclization (reaction S3.2) to form an (S∴N)-bonded multi-membered radical cation because of its relevance for peptide-chain dynamics. If the $>S^{\bullet+}{}_{NH2}$ radical cation (see its structure in Scheme 3) site cannot find the deprotonated amino group at the other end of the molecule in time to form an (S∴N) cyclic radical cation (SN notation in Scheme 3), then the $>S^{\bullet+}{}_{NH2}$ radical cation itself would be free to undergo typical reactions expected for monomeric sulfur radical cations $>S^{\bullet+}{}_{NH3+}$ (see its structure in Schemes 2 and 3) that are located in peptides with protonated amino groups. Such typical sulfur radical cationic reactions are deprotonation leading to the α-(alkylthio)alkyl radicals (αS) (S3.6a/b), formation of cyclic (S∴O)-bonded six-membered radicals at the C-terminal (S3.7), and intramolecular electron transfer (pseudo-Kolbe mechanism) leading to substituted amino radicals (αN_{subst}) (S3.8). In addition, these particular $>S^{\bullet+}{}_{NH2}$ radical cations could possibly undergo protonation of the N-terminal amino group by bulk protons (S3.5).

The rate constants for these processes can be estimated by using a 'radical clock'. Here the radical clock is the SO radical.[83] As previously argued,[41,42] the rate of formation of cyclic (S∴O)-bonded six-membered radicals is not expected to vary directly with the number of Pro residues in the bridges and with pH. So, this formation rate is the same as that determined from pulse radiolysis[41] and flash photolysis[42] experiments with Met-(Pro)$_n$-Met peptides, i.e., 7.7×10^5 s^{-1}.

With this cyclization rate of (S∴O)-bonded radicals, formation rates of αN_{subst} and αS radicals can be estimated from the following considerations. Based on the lack of SOH radicals and the simulations shown in Figure S8 together with the associated Comment S2 in the Supporting Information, the conjecture can be made that the initially formed $>S^{\bullet+}{}_{NH2}$ is the sole product formed from the SOH radical in peptides with n = 0, 1, and 2 Pro residues. Furthermore, given that the $>S^{\bullet+}{}_{NH2}$ radical is decaying competitively into the five channels above, including (S∴N) cyclic radical formation (SN notation in Scheme 3), it can be noted from Table 1 that three of the channels S3.6a/b, S3.7, and S3.8 have roughly the same yields for each of the peptides with n = 0, 1, and 2 Pro residues. Because the $>S^{\bullet+}{}_{NH2}$ radical decays competitively into five channels, the approximately equal yields of three of them (S3.6a/b, S3.7, and S3.8) means that these three channels also have roughly the same rates of formation starting from the decay of $>S^{\bullet+}{}_{NH2}$. Taking the rate of all three processes S3.6a/b, S3.7, and S3.8, the same as the cyclization of $>S^{\bullet+}{}_{NH2}$ to form (S∴O)-bonded radicals (S3.7), the resulting sum of these three decay processes of $>S^{\bullet+}{}_{NH2}$ is 2.3×10^6 s^{-1} ≈ $k_{S3.6a/b} + k_{S3.7} + k_{S3.8}$.

Of the remaining two decay processes of $>S^{\bullet+}{}_{NH2}$, it can be shown that one of them, the rate of protonation of $>S^{\bullet+}{}_{NH2}$ by bulk protons (S3.5), is insignificant compared to the sum (2.3×10^6 s^{-1}) of the abovementioned three. The proof is as follows: as before, we first note that the protonation reaction S3.5 is not pseudo-first order at pH 5.5. However, the rate can be computed using the same general formula for the half-life as in Comment S1 of the Supporting Information, but now taking the bulk water protonation rate constant to be the same as that with ammonia, 4.3×10^{10} M^{-1} s^{-1}.[82] The result is ~1×10^5 s^{-1} (see the details in Comment S3 of the Supporting Information). This constitutes the upper limit for the protonation rate constant for the N-terminal amino group in the oxidized γ-Glu-(Pro)$_n$-Met peptides by the bulk protons under our conditions. If this protonation rate is compared to the sum of the three formation rates of S3.6a/b, S3.7, and S3.8, the contribution of the protonation rate to the sum of these particular four rates of decay of $>S^{\bullet+}{}_{NH2}$ is only 4%. So, this process is taken as zero. This justifies the assumption that the decay of $>S^{\bullet+}{}_{NH2}$ can be treated as a simple competition of irreversible decays (Scheme 3), and Scheme 2 is irrelevant for the peptides with n = 0, 1, and 2 Pro residues.

Using the results of the above analysis, estimates of the overall rate constants of cyclization to form the (S∴N)-bonded multi-membered radical cation (SN notation in Scheme 3) can be made from the branching ratios for the main four $>S^{\bullet+}{}_{NH2}$ decay channels (eq 7). The details of the calculation and the derivation of eq 7 are in Comment S4 of the Supporting Information:

$$k_{S3.2} = (k_{S3.6a/b} + k_{S3.7} + k_{S3.8})\Phi/(1 - \Phi) \quad (7)$$

where

$$\Phi = G(\alpha N)/G(S^{\bullet+}{}_{NH2})$$

to give $k_{S3.2} = 3.8 \times 10^6$, 1.8×10^6, and 8.1×10^5 s^{-1} for n = 0, 1, and 2, respectively. This shows the explicit distance dependence of the cyclization reaction involving the $>S^{\bullet+}{}_{NH2}$ radical cations forming (S∴N)-bonded multi-membered radical cations (N-terminal).

3.3.4. Kinetics of Cyclization Reaction and Decarboxylation when n = 3. For the peptide γ-Glu-(Pro)$_3$-

https://dx.doi.org/10.1021/acs.jpcb.0c04371
J. Phys. Chem. B 2020, 124, 8082−8098

Met, the SOH radical was observed in the 340 nm trace of Figure 2 for several microseconds. This indicates the absence of an effective intramolecular proton transfer to promote the elimination of water from SOH radicals such as seen in γ-Glu-$(Pro)_n$-Met peptides with n = 0, 1, and 2. It is an indication that the other decay mechanisms for SOH radical, displayed in Scheme 2, were active in the peptide with n = 3.

It was shown above that bulk protonation reaction S3.5 of $>S^{\bullet+}{}_{NH2}$ was unlikely to allow for radical populations to progress from Scheme 3 to Scheme 2 for pH 5.5. In addition, the deprotonation reaction of $>S^{\bullet+}{}_{NH3+}$ in the equilibrium S3.5 is very slow. The rate of this reaction can be computed by elementary methods after assuming pK_a = 9.47 of $>S^{\bullet+}{}_{NH3+}$ is the same as that of the native peptide and that the protonation rate constant of $>S^{\bullet+}{}_{NH2}$ is the same as that of ammonia in water. The rate constant for the deprotonation reaction in equilibrium S3.5 was calculated to be ~15 s^{-1} (see Comment S5 in the Supporting Information). In effect, these two estimates for the rates of bulk protonation of $>S^{\bullet+}{}_{NH2}$ and deprotonation rates of $>S^{\bullet+}{}_{NH3+}$ associated with S3.5 show that Schemes 2 and 3 are isolated at the level of the sulfur radical cations in the mechanism.

This partitioning of Schemes 2 and 3 indicates that reaction S2.2 is mainly responsible for the relative long lifetime of SOH radicals in the peptide with n = 3, yet reaction S3.1 must still be responsible for the cyclization, the formation of SN radical cations, and the subsequent decarboxylation of the N-terminal group. So, it is the competition between the reactions S2.2 and S3.1 for the decay of SOH radicals that controls the N-terminal decarboxylation in the γ-Glu-$(Pro)_n$-Met peptide with n = 3.

In contrast to the approximate equality of the G values of SO, αS, and αN_{subst} radicals in the γ-Glu-$(Pro)_n$-Met peptides for n = 0, 1, 2, the G value of αS radicals in the peptide with n = 3 is distinctly larger than the G values of SO and αN_{subst} radicals for the n = 3 peptide. As argued above, the difference between the shorter peptides and the peptide with n = 3 is that the main reaction pathway goes through the sulfur radical cation with an unprotonated N-terminal amino group ($>S^{\bullet+}{}_{NH2}$) for γ-Glu-$(Pro)_n$-Met (n = 0, 1, 2), whereas the main reaction pathway goes through the sulfur radical cation with a protonated N-terminal amino group ($>S^{\bullet+}{}_{NH3+}$) for n = 3. This difference is likely the source of the enhanced $G(\alpha S)$ value relative to $G(SO)$ and $G(\alpha N_{subst})$ values for the n = 3 peptide. From the Met-$(Pro)_n$-Met work,[41,42] the (S.∴O)-cyclization rate was 7.7×10^5 s^{-1} as mentioned above, and the αS formation rate was 1.3×10^6 s^{-1}. It was shown by Bobrowski *et al.*[48] that protonation of the amino group enhances deprotonation from the carbon atoms immediately adjacent to the sulfur radical cationic site with the consequence of enhanced formation of αS radicals. Although the ratio of the rate for αS radical formation vs the rate of (S.∴O) cyclization in the Met-$(Pro)_n$-Met peptides is not sufficient to account quantitatively for the enhancement of the ratios of $G(\alpha S)/G(SO)$ and $G(\alpha S)/G(\alpha N_{subst})$ for γ-Glu-$(Pro)_3$-Met, the trend goes in the expected direction.

3.4. Differences in Trends of Efficiency and Kinetics of Intramolecular-Contact Formation between Remote Functional Groups in Met-$(Pro)_n$-Met and γ-Glu-$(Pro)_n$-Met Peptides. Interestingly, contrary to Met-$(Pro)_n$-Met (n = 0−4) peptides where the decrease of the radiation-chemical yields or quantum yields of intramolecularly S.∴S-bonded radical cations $(S.\therefore S)^+$ with the number (n) of proline residues was not linear,[41,42] the radiation-chemical yield of αN radicals in γ-Glu-$(Pro)_n$-Met (n = 0−3) peptides shows a linear decrease with the number (n) of proline residues (Figure 5).

In the first family of peptides, Met-$(Pro)_n$-Met (n = 0−4), there was a very weak decrease in the radiation-chemical yields or quantum yields of $(S.\therefore S)^+$ radical cations in peptides with 0−2 Pro residues. However, when the number of Pro residues was changed from 2 to 3, there was a larger change. This change was rationalized by contrasting dynamics. Reactive contact between the S-atoms in the terminal Met residues in the peptides with 0−2 Pro residues was controlled only by the activated formation of intramolecular $(S.\therefore S)^+$, whereas in the peptides with 3 and 4 Pro residues, by the relative diffusion of the $>S^{\bullet+}$ and unoxidized S-atom.[42] In turn, in γ-Glu-$(Pro)_n$-Met (n = 0−3) peptides, the decrease of the radiation-chemical yield of intramolecularly (S.∴N)-bonded multi-membered radical cation (SN notation in Scheme 3) (measured by the radiation-chemical yield of αN radicals) was constant (0.09 $\mu M\ J^{-1}$) with each added Pro residue. Since the rate of activated formation of intramolecular SN radical cations can be taken as constant for all of the γ-Glu-$(Pro)_n$-Met peptides, by analogy with Met-$(Pro)_n$-Met,[41] the observed permanent and continuous lowering of $G(\alpha N)$ with the number of Pro residues (from 0 to 3) suggests that the formation of a contact between the S-atom in the C-terminal Met residue and the N-atom (located in the deprotonated N-terminal amino group of the Glu-residue) is controlled in peptides with 0 to 3 Pro residues by the relative diffusion of the $S^{\bullet+}$ site and the N-atom. These diffusion-limited rates depend on the chain-diffusion coefficient that might reflect complex properties of polypeptide chains that determine the apparent end-to-end diffusion coefficients.

4. CONCLUSIONS

Our study concerns the folding of peptides with restricted conformational flexibility and develops a new probe for intramolecular contacts in peptides. In previous papers, such probes for intramolecular contacts included one for formation of a stable product (acetaldehyde) and one for the formation of intramolecularly S.∴S-bonded radical cations. Here, decarboxylation at the N-terminal of the peptides serves as another probe for intramolecular-contact formation.

We were able to estimate rate constants of intramolecular-contact formation between remote N-terminal amino groups in Glu residues and oxidized thioether groups in C-terminal Met residues in peptides with restricted conformational flexibility. These estimates came from our analysis of measured radiation-chemical yields of free radicals (αN, αN_{subst}, αS, and SO-bonded radicals) that were produced using $^{\bullet}$OH-induced oxidation at the C-terminal Met residue of γ-Glu-$(Pro)_n$-Met (n = 0−3) peptides. The $^{\bullet}$OH radical was used as a "radical trigger" that can initiate peptide/protein folding. It was shown that interactions between terminals of the oligopeptides can be successfully probed by the G values of αN radicals formed on the Glu residue. These αN radicals result from decarboxylation of intramolecularly SN-bonded radical cations. If the formation of these SN radical cations were not possible, then decarboxylation at the N-terminal of the peptides studied did not occur. The continuous decrease of $G(\alpha N)$ with the number of Pro residues indicates that the end-to-end contact formation was controlled by the relative diffusion within $>S^{\bullet+}{}_{NH2}$ between its unprotonated amino group and its sulfur radical cationic site. The overall rate constants of cyclization to

https://dx.doi.org/10.1021/acs.jpcb.0c04371
J. Phys. Chem. B 2020, 124, 8082−8098

form $(S.^{\cdot}.N)^{+}$ radical cations are a direct indication for the end-to-end dynamics along the chain.

Moreover, this study showed that a remote amino group that served as both a proton and a free-electron-pair donor and that was separated from Met residue by an oligoproline backbone could still affect the chemistry on Met. Therefore, oxidation reactions on Met may affect product patterns. Hydroxyl radicals or their metal-bound equivalents (perferryl species) are prominent oxidants under biological conditions of oxidative stress, including inflammatory reactions at injection sites of protein therapeutics.

■ ASSOCIATED CONTENT

Supporting Information

The Supporting Information is available free of charge at https://pubs.acs.org/doi/10.1021/acs.jpcb.0c04371.

(Figure S1) Three steps in spectral resolution procedure for the resolution of the spectral components in the transient absorption spectra recorded 8 μs after electron pulse following $^{\bullet}$OH-induced oxidation of γ-Glu-Met (0.2 mM) in N_2O-saturated aqueous solutions, pH = 5.3−5.6; (Figure S2) three steps in spectral resolution procedure for the resolution of the spectral components in the transient absorption spectra recorded 11 μs after electron pulse following $^{\bullet}$OH-induced oxidation of γ-Glu-Pro-Met (0.2 mM) in N_2O-saturated aqueous solutions, pH = 5.3−5.6; (Figure S3) three steps in spectral resolution procedure for the resolution of the spectral components in the transient absorption spectra recorded 7 μs after electron pulse following $^{\bullet}$OH-induced oxidation of γ-Glu-$(Pro)_2$-Met (0.2 mM) in N_2O-saturated aqueous solutions, pH = 5.3−5.6; (Figure S4) three steps in spectral resolution procedure for the resolution of the spectral components in the transient absorption spectra recorded 7 μs after electron pulse following $^{\bullet}$OH-induced oxidation of γ-Glu-$(Pro)_3$-Met (0.2 mM) in N_2O-saturated aqueous solutions, pH = 5.3−5.6; (Figure S5) reference spectra used in the resolutions of the transient absorption spectra following $^{\bullet}$OH-induced oxidation of γ-Glu-$(Pro)_n$-Met (0.2 mM) (n = 0−3); (Figure S6) reference spectrum of αN_{subst} radicals used in resolutions of the transient absorption spectra following $^{\bullet}$OH-induced oxidation of γ-Glu-$(Pro)_n$-Met (0.2 mM); (Figure S7) kinetics of PNAP radical anion formation after $^{\bullet}$OH-induced oxidation of γ-Glu-$(Pro)_n$-Met (0.2 mM) (n = 0−3) by PNAP (p-nitroacetophenone) (3×10^{-5} M) in N_2O-saturated aqueous solutions, pH ≈ 5.4: all kinetic traces are corrected for the background radical absorption at 360 nm; (Figure S8) simulations to find the lower limits of $k_{3.1}$; (Comment S1) estimation of a half-life of SOH in terms of its reaction with external (bulk) protons; (Comment S2) simulations to find the lower limits of $k_{3.1}$; (Comment S3) estimation of a half-life of the $>S^{\bullet+}_{NH2}$ in terms of its reaction with external (bulk) protons; (Comment S4) derivation of eq 7; and (Comment S5) estimation of deprotonation rate k_a of $S^{\bullet+}_{NH3+}$ in equilibrium S3.5 (PDF)

■ AUTHOR INFORMATION

Corresponding Author

Piotr Filipiak − *Faculty of Chemistry and Center for Advanced Technology, Adam Mickiewicz University, 61-614 Poznan, Poland;* orcid.org/0000-0001-9141-2163; Phone: +48 61 829-1738; Email: piotrf@amu.edu.pl; Fax: +48 61 829-1555

Authors

Krzysztof Bobrowski − *Institute of Nuclear Chemistry and Technology, 03-195 Warsaw, Poland; Radiation Laboratory, University of Notre Dame, Notre Dame, Indiana 46556, United States;* orcid.org/0000-0002-7791-9184

Gordon L. Hug − *Faculty of Chemistry, Adam Mickiewicz University, 61-614 Poznan, Poland; Radiation Laboratory, University of Notre Dame, Notre Dame, Indiana 46556, United States*

Christian Schöneich − *School of Pharmacy, Department of Pharmaceutical Chemistry, University of Kansas, Lawrence, Kansas 66047, United States;* orcid.org/0000-0001-5082-8672

Bronislaw Marciniak − *Faculty of Chemistry and Center for Advanced Technology, Adam Mickiewicz University, 61-614 Poznan, Poland;* orcid.org/0000-0001-8396-0354

Complete contact information is available at: https://pubs.acs.org/10.1021/acs.jpcb.0c04371

Author Contributions

K.B., B.M., P.F., and C.S. conceptualized the study. K.B., G.L.H., P.F., and B.M. conducted formal analysis. B.M. and P.F. acquired funding. C.S. performed the synthesis. P.F., K.B., and G.L.H. performed the investigation. P.F., K.B., G.L.H., and B.M. constructed the methodology. K.B. and B.M. performed validation. K.B., P.F., and G.L.H. prepared the original draft. K.B., P.F., B.M., G.L.H., and C.S. reviewed and edited the manuscript.

Funding

This research was funded by the National Science Centre Poland within grant nos. UMO-2013/11/B/ST4/00811 and UMO-2017/27/B/ST4/00375 and by the U.S. Department of Energy Office of Science, Office of Basic Energy Science under award number DE-FC02-04ER15533.

Notes

The authors declare no competing financial interest.

■ ACKNOWLEDGMENTS

P.F. and B.M. acknowledge the National Science Centre Poland for financial support mentioned above. Two of us (P.F. and K.B.) would like to acknowledge the NDRL accelerator staff and personally Professor Ian Carmichael for his hospitality during their stay at Notre Dame Radiation Laboratory. This is document number NDRL-5284 from the Notre Dame Radiation Laboratory.

■ REFERENCES

(1) Eaton, W. A.; Muñoz, V.; Hagen, S. J.; Jas, G. S.; Lapidus, L. J.; Henry, E. R.; Hofrichter, J. Fast kinetics and mechanisms in protein folding. *Annu. Rev. Biophys. Biomol. Struct.* **2000**, *29*, 327−359.

(2) Eaton, W. A.; Muñoz, V.; Thompson, P. A.; Henry, E. R.; Hofrichter, J. Kinetics and Dynamics of Loops, α-Helices, β-Hairpins, and Fast-Folding Proteins. *Acc. Chem. Res.* **1998**, *31*, 745−753.

(3) Eaton, W. A.; Thompson, P. A.; Chan, C.-K.; Hagen, S. J.; Hofrichter, J. Fast events in protein folding. *Structure* **1996**, *4*, 1133−1139.

(4) Telford, J. R.; Wittung-Stafshede, P.; Gray, H. B.; Winkler, J. R. Protein Folding Triggered by Electron Transfer. *Acc. Chem. Res.* **1998**, *31*, 755−763.
(5) Tremain, S. M. *Electron-transfer reactivity of metalloproteins in folded, partially unfolded, and completely unfolded forms*. Ph.D. Thesis. Iowa State University, 2002.
(6) Jennings, P. A.; Wright, P. E. Formation of a molten globule intermediate early in the kinetic folding pathway of apomyoglobin. *Science* **1993**, *262*, 892−896.
(7) Schindler, T.; Herrler, M.; Marahiel, M. A.; Schmid, F. X. Extremely rapid protein folding in the absence of intermediates. *Nat. Struct. Biol.* **1995**, *2*, 663−673.
(8) Kiefhaber, T. Kinetic traps in lysozyme folding. *Proc. Natl. Acad. Sci. U. S. A.* **1995**, *92*, 7292−9033.
(9) Yeh, S.-R.; Han, S.; Rousseau, D. L. Cytochrome c Folding and Unfolding: A Biphasic Mechanism. *Acc. Chem. Res.* **1998**, *31*, 727−736.
(10) Chan, C.-K.; Hu, Y.; Takahashi, S.; Rousseau, D. L.; Eaton, W. A.; Hofrichter, J. Submillisecond protein folding kinetics studied by ultrarapid mixing. *Proc. Natl. Acad. Sci. U. S. A.* **1997**, *94*, 1779−1784.
(11) Nolting, B.; Golbik, R.; Fersht, A. R. Submillisecond events in protein folding. *Proc. Natl. Acad. Sci. U. S. A.* **1995**, *92*, 10668−10672.
(12) Williams, S.; Causgrove, T. P.; Gilmanshin, R.; Fang, K. S.; Callender, R. H.; Woodruff, W. H.; Dyer, R. B. Fast Events in Protein Foldin: Helix Melting and Formation in a Small Peptide. *Biochemistry* **1996**, *35*, 691−697.
(13) Gruebele, M.; Sabelko, J.; Ballew, R.; Ervin, J. Laser Temperature Jump Induced Protein Refolding. *Acc. Chem. Res.* **1998**, *31*, 699−707.
(14) Phillips, C. M.; Mizutani, Y.; Hochstrasser, R. M. Ultrafast thermally induced unfolding of RNase A. *Proc. Natl. Acad. Sci. U. S. A.* **1995**, *92*, 7292−7296.
(15) Hofrichter, J. Laser temperature-jump methods for studying folding dynamics. *Methods Mol. Biol.* **2001**, *168*, 159−191.
(16) Dyer, R. B.; Gai, F.; Woodruff, W. H.; Gilmanshin, R.; Callender, R. H. Infrared Studies of Fast Events in Protein Folding. *Acc. Chem. Res.* **1998**, *31*, 709−716.
(17) Wirth, A. J.; Liu, Y.; Prigozhin, M. B.; Schulten, K.; Gruebele, M. Comparing Fast Pressure Jump and Temperature Jump Protein Folding Experiments and Simulations. *J. Am. Chem. Soc.* **2015**, *137*, 7152−7159.
(18) Ly, H. K.; Sezer, M.; Wisitruangsakul, N.; Feng, J.-J.; Kranich, A.; Millo, D.; Weidinger, I. M.; Zebger, I.; Murgida, D. H.; Hildebrandt, P. Surface-enhanced vibrational spectroscopy for probing transient interactions of proteins with biomimetic interfaces: electric field effects on structure, dynamics and function of cytochrome c. *FEBS J.* **2011**, *278*, 1382−1390.
(19) Marchioni, C.; Riccardi, E.; Spinelli, S.; Dell'Unto, F.; Grimaldi, P.; Bedini, A.; Giliberti, C.; Giuliani, L.; Palomba, R.; Castellano, A. C. Structural changes induced in proteins by therapeutic ultrasounds. *Ultrasonics* **2009**, *49*, 569−576.
(20) Jones, C. M.; Henry, E. R.; Hu, Y.; Chan, C.-K.; Luck, S. D.; Bhuyan, A.; Roder, H.; Hofrichter, J.; Eaton, W. A. Fast events in protein folding initiated by nanosecond laser photolysis. *Proc. Natl. Acad. Sci. U. S. A.* **1993**, *90*, 11860−11864.
(21) Hagen, S. J.; Hofrichter, J.; Szabo, A.; Eaton, W. A. Diffusion-limited contact formation in unfolded cytochrome c: Estimating the maximum rate of protein folding. *Proc. Natl. Acad. Sci. U. S. A.* **1996**, *93*, 11615−11617.
(22) Camacho, C. J.; Thirumalai, D. Theoretical predictions of folding pathways by using the proximity rule, with applications to bovine pancreatic trypsin inhibitor. *Proc. Natl. Acad. Sci. U. S. A.* **1995**, *92*, 1277−1281.
(23) Hagen, S. J.; Hofrichter, J.; Eaton, W. A. Rate of Intrachain Diffusion of Unfolded Cytochrome c. *J. Phys. Chem. B* **1997**, *101*, 2352−2365.
(24) Bieri, O.; Wirz, J.; Hellrung, B.; Schutkowski, M.; Drewello, M.; Kiefhaber, T. The speed limit for protein folding measured by triplet−triplet energy transfer. *Proc. Natl. Acad. Sci. U. S. A.* **1999**, *96*, 9597−9601.
(25) Lapidus, L. J.; Eaton, W. A.; Hofrichter, J. Measuring the rate of intramolecular contact formation in polypeptides. *Proc. Natl. Acad. Sci. U. S. A.* **2000**, *97*, 7220−7225.
(26) Lapidus, L. J.; Steinbach, P. J.; Eaton, W. A.; Szabo, A.; Hofrichter, J. Effects of Chain Stiffness on the Dynamics of Loop Formation in Polypeptides. Appendix: Testing a 1-Dimensional Diffusion Model for Peptide Dynamics. *J. Phys. Chem. B* **2002**, *106*, 11628−11640.
(27) Lapidus, L. J.; Eaton, W. A.; Hofrichter, J. Measuring Dynamic Flexibility of the Coil State of a Helix-forming Peptide. *J. Mol. Biol.* **2002**, *319*, 19−25.
(28) Szabo, A.; Schulten, K.; Schulten, Z. First passage time approach to diffusion controlled reactions. *J. Chem. Phys.* **1980**, *72*, 4350−4357.
(29) Ahmad, B.; Chen, Y.; Lapidus, L. J. Aggregation of α-synuclein is kinetically controlled by intramolecular diffusion. *Proc. Natl. Acad. Sci. U. S. A.* **2012**, *109*, 2336−2341.
(30) Srivastava, K. R.; French, K. C.; Tzul, F. O.; Makhatadze, G. I.; Lapidus, L. J. Intramolecular diffusion controls aggregation of the PAPf39 peptide. *Biophys. Chem.* **2016**, *216*, 37−43.
(31) Voelz, V. A.; Singh, V. R.; Wedemeyer, W. J.; Lapidus, L. J.; Pande, V. S. Unfolded-State Dynamics and Structure of Protein L Characterized by Simulation and Experiment. *J. Am. Chem. Soc.* **2010**, *132*, 4702−4709.
(32) Waldauer, S. A.; Bakajin, O.; Lapidus, L. J. Extremely slow intramolecular diffusion in unfolded protein L. *Proc. Natl. Acad. Sci. U. S. A.* **2010**, *107*, 13713−13717.
(33) Srivastava, K. R.; Lapidus, L. J. Prion protein dynamics before aggregation. *Proc. Natl. Acad. Sci. U. S. A.* **2017**, *114*, 3572−3577.
(34) Schöneich, C.; Zhao, F.; Madden, K. P.; Bobrowski, K. Side chain fragmentation of N-terminal threonine or serine residue induced through intramolecular proton transfer to hydroxy sulfuranyl radical formed at neighboring methionine in dipeptides. *J. Am. Chem. Soc.* **1994**, *116*, 4641−4652.
(35) Pogocki, D.; Ghezzo-Schöneich, E.; Schöneich, C. Conformational Flexibility Controls Proton Transfer between the Methionine Hydroxy Sulfuranyl Radical and the N-Terminal Amino Group in Thr-$(X)_n$-Met Peptides. *J. Phys. Chem. B* **2001**, *105*, 1250−1259.
(36) Bobrowski, K.; Schöneich, C.; Holcman, J.; Asmus, K.-D. $^{\bullet}$OH radical induced decarboxylation of γ-glutamylmethionine and S-alkylglutathione derivatives: Evidence for two different pathways involving C- and N-terminal decarboxylation. *J. Chem. Soc., Perkin Trans. 2* **1991**, 975−980.
(37) Bobrowski, K.; Schöneich, C. Decarboxylation mechanism of the N-terminal glutamyl moiety in γ-glutamic acid and methionine containing peptides. *Radiat. Phys. Chem.* **1996**, *47*, 507−510.
(38) Bobrowski, K.; Hug, G. L.; Pogocki, D.; Marciniak, B.; Schöneich, C. Sulfur radical cation peptide bond complex in the one-electron oxidation of S-methylglutathione. *J. Am. Chem. Soc.* **2007**, *129*, 9236−9245.
(39) Bobrowski, K.; Holcman, J. Formation and stability of intramolecular three-electron S∴N, S∴S, and S∴O bonds in one-electron-oxidized simple methionine peptides Pulse radiolysis study. *J. Phys. Chem.* **1989**, *93*, 6381−6387.
(40) Bobrowski, K.; Hug, G. L.; Pogocki, D.; Marciniak, B.; Schöneich, C. Stabilization of sulfide radical cations through complexation with the peptide bond: mechanisms relevant to oxidation of proteins containing multiple methionine residues. *J. Phys. Chem. B* **2007**, *111*, 9608−9620.
(41) Filipiak, P.; Bobrowski, K.; Hug, G. L.; Pogocki, D.; Schöneich, C.; Marciniak, B. Formation of a Three-Electron Sulfur−Sulfur Bond as a Probe for Interaction between Side Chains of Methionine Residues. *J. Phys. Chem. B* **2016**, *120*, 9732−9744.
(42) Filipiak, P.; Bobrowski, K.; Hug, G. L.; Pogocki, D.; Schöneich, C.; Marciniak, B. New Insights into the Reaction Paths of 4-Carboxybenzophenone Triplet with Oligopeptides Containing N- and

https://dx.doi.org/10.1021/acs.jpcb.0c04371
J. Phys. Chem. B 2020, 124, 8082−8098

C-Terminal Methionine Residues. *J. Phys. Chem. B* **2017**, *121*, 5247−5258.
(43) He, S.; Scheraga, H. A. Brownian dynamics simulations of protein folding. *J. Chem. Phys.* **1998**, *108*, 287−300.
(44) Pizzorno, J. Glutathione! *Integrative Medicine* **2014**, *13*, 8−12.
(45) Elango, N.; Janaki, S.; Rao, A. R. Two Affinity chromatography methods for purification of glyoxylase I from rabbit liver. *Biochem. Biophys. Res. Comms.* **1978**, *83*, 1388−1395.
(46) Del Boccio, G.; Pennelli, A.; Whitehead, E. P.; Lo Bello, M.; Petruzzelli, R.; Federici, G.; Ricci, G. Interaction of glutathione transferaze from horse erythrocytes with 7-chloro-4-nitrobenzo-2-oxa1,3-diazole. *J. Biol. Chem.* **1991**, *266*, 13777−13782.
(47) Jenei, Z.; Janáky, R.; Varga, V.; Saransaari, P.; Oja, S. S. Interference of S-alkyl derivatives of glutathione with brain ionotropic glutamate receptors. *Neurochem. Res.* **1998**, *23*, 1085−1091.
(48) Bobrowski, K.; Schöneich, C.; Holcman, J.; Asmus, K.-D. $^{\bullet}$OH radical induced decarboxylation of methionine-containing peptides. Influence of peptide sequence and net charge. *J. Chem. Soc., Perkin Trans. 2* **1991**, 353−362.
(49) Filipiak, P.; Hug, G. L.; Bobrowski, K.; Pedzinski, T.; Kozubek, H.; Marciniak, B. Sensitized Photooxidation of S-Methylglutathione in Aqueous Solution: Intramolecular (S∴O) and (S∴N) Bonded Species. *J. Phys. Chem. B* **2013**, *117*, 2359−2368.
(50) Sridharan, U.; Ponnuraj, K. Isopeptide bond in collagen- and fibrinogen-binding MSCRAMMs. *Biophys Rev* **2016**, *8*, 75−83.
(51) De Jong, G. A. H.; Koppelman, S. J. Transglutaminase Catalyzed Reactions: Impact on Food Applications. *J. Food Sci.* **2002**, *67*, 2798−2806.
(52) Beck, A.; Bussat, M.-C.; Klinguer-Hamour, C.; Goetsch, L.; Aubry, J.-P.; Champion, T.; Julien, E.; Haeuw, J.-F.; Bonnefoy, J.-Y.; Corvaia, N. Stability and CTL activity of N-terminal glutamic acid containing peptides. *J. Peptide Res.* **2001**, *57*, 528−538.
(53) Chelius, D.; Jing, K.; Lueras, A.; Rehder, D. S.; Dillon, T. M.; Vizel, A.; Rajan, R. S.; Li, T.; Treuheit, M. J.; Bondarenko, P. V. Formation of Pyroglutamic Acid from N-Terminal Glutamic Acid in Immunoglobulin Gamma Antibodies. *Anal. Chem.* **2006**, *78*, 2370−2376.
(54) Honegger, A.; Plückthun, A. Yet Another Numbering Scheme for ImmunoglobulinVariable Domains: An Automatic Modeling and Analysis Tool. *J. Mol. Biol.* **2001**, *309*, 657−670.
(55) Zhang, Z.; Henzel, W. J. Signal peptide prediction based on analysis of experimentally verified cleavage sites. *Protein Sci.* **2004**, *13*, 2819−2824.
(56) Hug, G. L.; Wang, Y.; Schöneich, C.; Jiang, P.-Y.; Fessenden, R. W. Multiple time scales in pulse radiolysis. Application to bromide solutions and dipeptides. *Radiat. Phys. Chem.* **1999**, *54*, 559−566.
(57) Buxton, G. V. An overview of the radiation chemistry of liquids. In *Radiation Chemistry: From Basics to Applications in Material and Life Sciences*; Spotheim-Maurizot, M., Mostafavi, M., Douki, T., Belloni, J., Eds.; EDP Sciences, 2008; pp. 3−16.
(58) Buxton, G. V.; Greenstock, C. L.; Helman, W. P.; Ross, A. B. Critical review of rate constants for reactions of hydrated electrons, hydrogen atoms and hydroxyl radicals ($^{\bullet}$OH/O$^{\bullet-}$) in aqueous solution. *J. Phys. Chem. Ref. Data* **1988**, *17*, 513−886.
(59) Schuler, R. H.; Hartzell, A. L.; Behar, B. Track effects in radiation chemistry. Concentration dependence for the scavenging of OH by ferrocyanide in N_2O-saturated aqueous solutions. *J. Phys. Chem.* **1981**, *85*, 192−199.
(60) Janata, E.; Schuler, R. H. Rate constant for scavenging eaq- in Nitrous oxide-saturated solutions. *J. Phys. Chem.* **1982**, *86*, 2078−2084.
(61) Marciniak, B.; Bobrowski, K.; Hug, G. L. Quenching of triplet states of aromatic ketones by sulfur-containing amino acids in solution. Evidence for electron transfer. *J. Phys. Chem.* **1993**, *97*, 11937−11943.
(62) Hiller, K.-O.; Asmus, K.-D. Tl^{2+} and Ag^{2+} metal-ion-induced oxidation of methionine in aqueous solution. A pulse radiolysis study. *Int. J. Radiat. Biol. Relat. Stud. Phys., Chem. Med.* **1981**, *40*, 597−604.
(63) Hug, G. L.; Bobrowski, K.; Pogocki, D.; Hörner, G.; Marciniak, B. Conformational influence on the type of stabilization of sulfur radical cations in cyclic peptides. *ChemPhysChem* **2007**, *8*, 2202−2210.
(64) Schöneich, C.; Pogocki, D.; Hug, G. L.; Bobrowski, K. Free radical reactions of methionine in peptides: mechanisms relevant to β-amyloid oxidation and Alzheimer's disease. *J. Am. Chem. Soc.* **2003**, *125*, 13700−13713.
(65) Bobrowski, K.; Hug, G. L.; Marciniak, B.; Miller, B.; Schöneich, C. Mechanism of one-electron oxidation of β-, γ-, and δ-hydroxyalkyl sulfides Catalysis through intramolecular proton transfer and sulfur-oxygen bond formation. *J. Am. Chem. Soc.* **1997**, *119*, 8000−8011.
(66) Steffen, L. K.; Glass, R. S.; Sabahi, M.; Wilson, G. S.; Schöneich, C.; Mahling, S.; Asmus, K. D. OH radical induced decarboxylation of amino acids. Decarboxylation vs bond formation in radical intermediates. *J. Am. Chem. Soc.* **1991**, *113*, 2141−2145.
(67) Schöneich, C.; Bobrowski, K. Intramolecular hydrogen transfer as the key step in the dissociation of hydroxyl radical adducts of (alkylthio)ethanol derivatives. *J. Am. Chem. Soc.* **1993**, *115*, 6538−6547.
(68) Hayon, E.; Ibata, T.; Lichtin, N. N.; Simic, M. Sites of Attack of Hydroxyl Radicals on Amides in Aqueous Solution. *J. Am. Chem. Soc.* **1970**, *92*, 3898−3903.
(69) Bonifacic, M.; Schaefer, K.; Moeckel, H.; Asmus, K.-D. Primary Steps in the Reactions of Organic Disulfides with Hydroxyl Radicals in Aqueous Solution. *J. Phys. Chem.* **1975**, *79*, 1496−1502.
(70) Wiśniowski, P.: *Influence of neighboring functional groups on radiation-induced radical processes in thioethers*. Ph.D. Thesis. Institute of Nuclear Chemistry and Technology, 2001.
(71) Bobrowski, K.; Pogocki, D.; Schöneich, C. Oxidation of (carboxyalkyl)-thiopropionic acid derivatives by hydroxyl radicals. Mechanisms and kinetics of competitive inter- and intramolecular formation of σ- and σ*-type sulfuranyl radicals. *J. Phys. Chem. A* **1998**, *102*, 10512−10521.
(72) Asmus, K.-D. Sulfur-centered three-electron bonded radical species. In *Sulfur-Centered Reactive Intermediates in Chemistry and Biology*; Chatgilialoglu, C., Asmus, K.-D., Eds.; Plenum Press: New York, 1990; Vol. *197*; pp. 155−172.
(73) Glass, R. S. Neighbouring group participation: General principles and application to sulfur-centered reactive species. In *Sulfur-centered reactive intermediates in chemistry and biology*; Chatgilialoglu, C., Asmus, K.-D., Eds.; Plenum Press: New York, 1990; Vol. *97*; pp. 213-.
(74) Glass, R. S. Sulfur radical cations. *Top. Curr. Chem.* **1999**, *205*, 1−87.
(75) Hiller, K. O.; Asmus, K. D. Formation and reduction reactions of α-amino radicals derived from methionine and its derivatives in aqueous solutions. *J. Phys. Chem.* **1983**, *87*, 3682−3688.
(76) Fu, Y.; Liu, L.; Yu, H.-Z.; Wang, Y.-M.; Guo, Q.-X. Quantum-Chemical Predictions of Absolute Standard Redox Potentials of Diverse Organic Molecules and Free Radicals in Acetonitrile. *J. Am. Chem. Soc.* **2005**, *127*, 7227−7234.
(77) Pogocki, D. M. *Investigation of radical processes induced by hydroxyl radical in amino acids and peptides containing thioether group*. Ph.D. Thesis. Institute of Nuclear Chemistry and Technology, 1996.
(78) Meisel, D.; Neta, P. One-electron redox potentials of nitro compounds and radiosensitizers. Correlation with spin densities of their radical anions. *J. Am. Chem. Soc.* **1975**, *97*, 5198−5203.
(79) Adams, G. E.; Willson, R. E. Ketyl radicals in aqueous solution. Pulse radiolysis study. *J. Chem. Soc., Faraday Trans. I* **1973**, *69*, 719−729.
(80) Domazou, A. S.; Zelenay, V.; Koppenol, W. H.; Gebicki, J. M. Efficient depletion of ascorbate by amino acid and protein radicals under oxidative stress. *Free Radical Biol. Med.* **2012**, *53*, 1565−1573.
(81) Braiman, M. S.; Mogi, T.; Marti, T.; Stern, L. J.; Khorana, G.; Rotschild, K. J. Vibrational Spectroscopy of Bacteriorhodopsin Mutants: Light-Driven Proton Transport Involves Protonation Changes of Aspartic Acid Residues 85, 96, and 212. *Biochemistry* **1988**, *27*, 8516−8520.

https://dx.doi.org/10.1021/acs.jpcb.0c04371
J. Phys. Chem. B 2020, 124, 8082−8098

(82) Eigen, M. Proton Transfer, Acid-Base Catalysis, and Enzymatic Hydrolysis, Part I: ELEMENTARY PROCESSES. *Angew. Chem., Int. Ed. Engl.* **1964**, *3*, 1−19.
(83) Newcomb, M. Radical Kinetics and Clocks. In *Encyclopedia of Radicals in Chemistry, Biology and Materials*; Chatgilialoglu, C., Studer, A., Eds.; John Wiley & Sons, 2012; Vol. *1*.

https://dx.doi.org/10.1021/acs.jpcb.0c04371
J. Phys. Chem. B 2020, 124, 8082−8098